Benjamin Reeber

Techno-Economic Evaluation of CO$_2$-Selective Facilitated Transport Membranes for an IGCC Power Plant

Master's thesis in Chemical Engineering
Supervisor: Liyuan Deng
Co-supervisor: Arne Lindbråthen

June 2022

Master's thesis

NTNU
Norwegian University of
Science and Technology

Benjamin Reeber

Techno-Economic Evaluation of CO$_2$-Selective Facilitated Transport Membranes for an IGCC Power Plant

Master's thesis in Chemical Engineering
Supervisor: Liyuan Deng
Co-supervisor: Arne Lindbråthen
June 2022

Norwegian University of Science and Technology
Faculty of Natural Sciences
Department of Chemical Engineering

NTNU
Norwegian University of
Science and Technology

Abstract

The purpose of this thesis is to present a techno-economic analysis of facilitated transport hollow-fiber membranes for H_2 purification and carbon capture at an integrated gasification combined cycle power plant.

Two membrane process configurations for separating H_2 and CO_2 were analyzed in an IGCC power plant application. The process flowsheet was developed in Aspen HYSYS based off available process data for a 634 MW gross power plant. The capital and operating costs for each configuration comprising compressors, drives, heat exchangers, vessels, and membranes were then calculated using a module-based costing approach. Several variables within each process configuration, such as sweep flow, recycle pressure, recompression pressure, were varied to analyze their effect on key financial metrics indicating the cost of electricity and required CO_2 processing incentives for the project to be viable. A sensitivity analysis was conducted on further variables including the membrane cost and discount rate to determine the impact these factors have on the project financial metrics.

At 90% CO_2 capture, a levelized cost of electricity of $143.99, or a 33% increase over the base case, is determined to be the lowest cost of electricity for the cases tested, with a breakeven CO_2 penalty of $128.19 per metric ton. These metrics compare similarly to the established adsorption technology, which captures 90% of carbon emissions at a 31% increase in levelized cost of electricity.

Sammendrag

Formålet med denne avhandlingen er å presentere en teknoøkonomiskanalyse av fasilliterttransport hulfibermembraner for H2-rensing og karbonfangst for et integrert gassifiserings- kombinertsykluskraftverk.

To membranprosesskonfigurasjoner for separering av CO2 og H2 ble analysert for en IGCC-kraftverksapplikasjon. Prosessflytskjemaet ble utviklet i Aspen HYSYS, basert på tilgjengelige prosessdata for et 634 MW brutto kraftverk. Kapital- og driftskostnadene for hver konfigurasjon bestående av kompressorer, motorer, varmevekslere, tanker og membraner ble deretter beregnet ved hjelp av en modulbasert kosttilnærming.

Flere variabler innenfor hver prosesskonfigurasjon, for eksempel sweep-strøm, resirkuleringstrykk, rekompresjonstrykk, ble varierte for å analysere effekten av disse på viktige økonomiske beregninger. Dette gir indikasjoner på kostnadsnivået for elektrisitet og nødvendige CO2-prosesseringsinsentiver for at prosjektet skal være levedyktig. Det ble gjennomført en sensitivitetsanalyse av ytterligere variabler også, inkludert membrankostnad og diskonteringssats for å fastslå hvilken innvirkning disse faktorene har på prosjektets økonomiske beregninger.

Ved 90% CO2-fangst er en strømkostnad på $ 143,99, eller en 33% økning over basiskassen, bestemt til å være den laveste kostnaden på elektrisitet for de testede senariene. Dette gir en breakeven CO2-kostnad på $ 128,19 per tonn. Disse beregningene sammenligner seg godt med den mest etablerte adsorpsjonsteknologien, som fanger 90 % av karbonutslippene med en 31 % økning av strømkostnaden.

Preface

This thesis is the culmination of my work in the Master of Science in Chemical Engineering (MSCHEMENG) in the department of Chemical Engineering (IKP) at the Norwegian University of Science & Technology (NTNU). This is a continuation of the specialization project started in the fall of 2021.

As old habits are sometime hard to change, unless otherwise noted, the period "." is used as the decimal separator, while the comma, "," is used to separate the thousands place in this report.

Contents

List of Figures

List of Tables

List of Abbreviations and Symbols

ε	Surface porosity
η	Viscosity
τ	Pore tortuosity
$	United States Dollar
€	Euro
A	Area
Adj	Adjust
AGR	Acid gas removal
CB&I	Chicago Bridge & Iron
CCC	Cost of carbon capture
C_{MR}	Cost of membrane replacement
C_{OL}	Cost of operating labor
CO_2	Carbon Dioxide
COM	Cost of manufacture
COS	Carbonyl Sulfide
C_{UT}	Cost of utilities
D	Diffusivity
EU	European Union
F	Fahrenheit
FCI	Full capital investment
GPU	Gas permeation units
H_2	Hydrogen
H_2S	Hydrogen sulfide
HCl	Hydrochloric acid
Hg	Mercury
IGCC	Integrated gasification combined cycle
J	Flux
L	Length
LCOE	Levelized cost of electricity
LHV	Lower heating value
m	Meter
MM	Million
MTR	Membrane Technology and Research
MWhr	Megawatt hour
N	Years of project life
NETL	National Energy Technology Laboratory (US)

NO_x	Nitrous oxides
NSPS	New Source Performance Standards
NTNU	Norwegian University of Science & Technology
OL	Operating lifetime
P	Pressure
PM	Particulate matter
Psig	Pounds per square inch, gauge
Ppm	Parts per million
PVA	Poly (vinyl alcohol)
Q	Heat Flux
r	Radius
S	Solubility
SCFD	Standard cubic foot per day
SLM	Supported liquid membranes
Sm^3	Standard cubic meter
SO_x	Sulfur Oxides
t	Metric tonne
U	Overall heat transfer coefficient
US DOE	United States Department of Energy

1 Background

1.1 Introduction

Elevated levels of carbon dioxide in the atmosphere are recognized as having human-generated sources and present a major challenge for human health and the environment [1]. While other anthropogenic greenhouse gases also contribute to climate change, Carbon Dioxide (CO_2) is the most emitted. Historically, CO_2 levels fluctuated, but did not rise above 300 parts per million (ppm) [2]. In 2020, the atmosphere levels of CO_2 averaged a dangerously high 412 ppm, with levels expected to continue to rise in the future.

Power generation is a significant source of carbon dioxide emissions. Of all fuel sources, coal is used to generated the most energy, totaling 39% of global power in 2015 [3]. Likewise, coal produced more CO_2 emissions than any other fuel source. Combustion exhaust, termed flue gases, from power generation are typically sent to the atmosphere without any removal or reduction of carbon dioxide content [4]. Previously, other pollutants like nitrous oxides (NO_x) and sulfur oxides (SO_x) were also emitted without any controls. As regulations and technologies improved over the past several decades, in many countries these pollutants have been regulated to be captured and are emitted in much smaller quantities today.

There are several potential pathways to a reduction in CO_2 emissions [5]. Reducing consumption of energy through energy-saving tactics or improved efficiencies of end uses would reduce CO_2 emitted. However, this would require changing attitudes and habits of consumers, which is not always easily or uniformly achieved. An alternative is that power generation technologies could be brought online to replace fossil-fuel based generation capacity. However, due to the large amount of fossil fuels currently used in the world, this would require considerable time, capital, and other resources.

A third approach is utilize carbon capture, which consists of preventing carbon from being emitted to the atmosphere [4]. In pre-combustion capture, the method is to remove the carbon from the fuel source prior to combustion [6]. If the carbon is removed, burning other components, like hydrogen, produce no CO_2 emissions. Typically, it is easiest to remove the carbon from the fuel in a gaseous state, so a synthesized gas, or syngas, is created from solid or liquid fuel. Another way that carbon can be captured is after combustion, by removing CO_2 from the flue gas emitted to the atmosphere [7]. The downside to capturing CO_2 from flue gas is that as most fuels are combusted in the presence of air, often with excess nitrogen, the CO_2 is often much lower in concentration and pressure than compared to the syngas approach. Oxyfuel combustion is the third method that can be used to capture carbon, by burning fuels in the presence of oxygen for a CO_2-rich flue gas that can be captured directly after combustion. Within each of these approaches, there are numerous variants on technologies and processes than can be employed.

After carbon dioxide is captured and concentrated into a gas stream, it needs to be processed further. The degree of processing depends on the final use and its

requirements for CO_2. Common processing steps include removing impurities such as water or sulfur, compression, and transport to the final usage or storage location.

As carbon dioxide levels reach record historic highs, carbon capture offers a pathway to slow the increase in carbon dioxide emissions [8]. Challenges related to energy consumption, safety, and potential impact on the environment have prevented carbon capture and storage technologies from becoming widely adopted [9]. Without any further action, emissions, and atmospheric carbon dioxide levels will continue to rise.

A membrane as defined by Mulder is a "Selective barrier between two phases, the term 'selective' being inherent to a membrane or membrane process" [10]. Membranes were first observed scientifically in the 18th century. The first experiments, undertaken by Nollet in the 1750's, observed that a pig's bladder can be used to induce a selective transfer of molecules [11]. Early experiments continued the trend of observing phenomena in natural materials, until in the 1860's Traube synthesized the first synthetic membrane.

In the 1920's, membranes began to be used more often in laboratory scale settings in Germany [10]. It was not until the 1950's and 1960's when membranes started to be used industrially for desalination. Over the past several decades, improvements in membrane technology have led to an increase in their importance and a wider range of applications. In several applications, membrane are critical components of separation processes. These include desalination, where reverse osmosis membranes are used to remove unwanted salts from water, the pharmaceutical industry, where membranes can be used to purify ingredients and separate desired products, the food industry, where macromolecules can be separated to reach the desired texture, and the chemical industry, where membranes can be used to separate out liquid or gaseous components. Membranes have been used in reverse osmosis plants capable of carrying over 300,000 m^3 per day, indicating a level of technological maturity in this field [4]. In natural gas processing, membrane systems capable of processing 250 MM SCFD ($7.08*10^6$ Sm^3 per day) have been installed, also indicating a level of technological maturity in gas phase applications [12]. The success from reverse osmosis and natural gas processing indicates a pathway for the spread of membranes to be more widely used in other separation processes.

That membranes are used in a wide range of applications today is testimony to the years of research and development of membarnes, along with the diverse array of materials that can be used to fabricate membranes. With each application, the properties of a membrane material and its interaction with the components that pass through it have an impact on the membrane's performance.

In recent years, membranes have been gaining increased styudy in the field of carbon capture and hydrogen purification [13]. Membrane separations have already been proven commercially viable in specific gas separtion processes, such as air seperation and the removal of acid gases including CO_2 and hydrogen sulfide (H_2S) from natural gas [14], [13]. Membranes can be comprised of different classes of materials, and many of these can be used for CO_2 separation applications. Polymer membranes are used across a broad range of gas separation applications. Polymer based membranes can be either glassy or ruberry. In the rubbery state, differences in solubility promotes the separation, while in the glassy state differences in permeability determine the transport throught the membrane. While polymers are ofter cheaper to fabricate, they have less stability at higher temperatures and pressures.

Facilitated transport membranes are a subcategory of membranes. The first studies with facilitated transport occurred in the 1960's[15]. After the discovery of improved polymeric membranes, little research was completed on facilitated transport membranes until the past few decades. Compared to basic polymer membranes, these have an additional transport mechanism in addition to the solution-diffusion that allows for faster transport of the desired components through the membrane. [13]. Initial facilitated transport membranes were supported liquid membranes (SLM), which relied on a liquid carrier within the membrane. Today, the class of faciltated transport membranes can be divided mostly into fixed and mobile carrier based membranes. obile carriers, contain a liquid carrier to faciltiate transport across the membrane. While this may lead to improved performance, the liquid also poses issues as there is both the potential for leakage of the mobile carrier and reduced membrane stability. There is also the potential for evaporation and environmental contamination. In fixed site membranes, the carrier is embedded into the polymer chain. This allows for increased mechanical stability due to the integration of the carrier within the membrane itself.

Membranes are particularly suited to applications with high concentrations of CO_2. Roussanaly and Anatharaman analyzed CO_2 avoidance cost with several different membranes at different CO_2 concentrations [16]. They found that when CO_2 capture ratios are set to 90%, membrane capture costs decrease when the concentration of CO_2 rises from 10% to 35%, the avoided cost of CO_2 drops from 64€/$t_{CO2\ avoided}$ to 15€/$t_{CO2\ avoided}$ [16]. Additionally, if lower carbon capture ratios are permitted, the cost of avoidance of CO_2 per ton are lowered further.

Several studies have examined the pre-combustion application of membrane separation to reduce carbon dioxide emissions. Grainger and Hägg suggested a three-stage CO_2 selective membrane process [17]. The proposed process utilized was a fixed site carrier polyvinyl amine membrane to achieve 95% pure compressed CO_2 with an 85% recovery rate, at a total cost of €40 per metric ton of CO_2.

Nagumo, et. al., analyzed both single and two stage membrane process for CO_2 capture in an IGCC power plant and found that the two-stage membrane process had a higher overall efficiency [18]. Above a selectivity of 30, further improvements in selectivity did not have a significant impact on the overall efficiency. In a two-stage process, higher recycle rates resulted in a lower overall efficiency. However, this work did not study other factors, such as purity or recovery of the final CO_2 or hydrogen (H_2) product streams.

Ku et. al analyzed the performance requirements of a H_2 selective membrane needed to achieve 90% H_2 recovery in a single-stage process. The authors found that with an assumed H_2 permeance of 1000 gas permeation units (GPU), H_2-selective membranes would need to have a selectivity of 62 [19]. This exceeded the upper performance limits of most membrane materials available at that time of the publication (2011).

Merkel, Zhou, and Baker provided a techno-economic analysis of MTR's membranes in different configurations [20]. The authors analyzed three different configurations combined with cryogenic distillation. A CO_2 selective, H_2 selective, and combination of the aforementioned membrane were included in their article. Several key assumptions were made in the report, including that H_2S can be co-sequestered with CO_2. However, H_2S guidelines today in the EU recommend a maximum H_2S concentration of 200 ppm[4]. This concentration is exceeded as the percentage ranges between 1.3%

15

and 1.4% in the final CO_2 product. However, if CO_2 is permitted to be co-injected with membranes, this could be a major advantage to membranes, as SO_x emissions generated from combustion could be reduced without further treatment, thereby removing a separation step from the power generation plant[20]. The authors note that an additional step to remove H_2S using the traditional method (a Selexol unit prior to the membrane) would add approximately 5% to the LCOE. Newer technologies for sulfur removal are also in development that could reduce the cost of this separation. The authors argue that cryogenic distillation in combination with membranes offer better performance than either technology alone. By including a membrane, the temperature of the cryogenic separation is able to be higher than it would be otherwise. Using the cryogenic separation prior to the membrane reduces the membrane area needed.

Merkel et al. indicated that improvements to membrane performance could be made to lower the LCOE from IGCC power plants. Their analysis was that based upon their designs, an H_2-selective membrane with a selectivity of 40 and a permanence of 900 GPU would come very close to meeting the US Department of Energy (DOE) target of a 10% increase in the levelized cost of electricity[20]. Merkel et. al. also notes that while the membrane area to capture CO_2 from modern full-scale IGCC power plants would be large, it is consistent with the scale of systems used in natural gas plants, which have ranged up to 50,000 m^2.

Another option explored in the Merkel paper is the use of a sweep gas, which is an additional gas stream use to dilute concentrations of solutes on the permeate side and increase flux through the membrane. Since nitrogen is present at 30 bars from the ASU (Air separation unit) in the plant as a byproduct of oxygen used in combustion, this could be used as a sweep gas. Furthermore, nitrogen is typically added to the combustion fuel to lower combustion temperatures and reduce NO_x formation, so after adding it to the gas stream during syngas separation it doesn't have to be removed later. In summary, three arguments are offered for the H_2-selective membrane over the CO_2 selective membrane [20]. Reduced initial syngas cooling from a higher operating temperature. Second, a drier CO_2 product due to permeation of water vapor through H_2-selective membrane. Lastly, nitrogen can be used as sweep gas to improve separation performance

However, an H_2-selective membrane with sweep is not without its limitations. The current capabilities of hydrogen selective membranes mean that there is a need for low temperature condensation to separate hydrogen in the distillation column, which ads to both and operating costs due to expensive metallurgy and high energy requirements from the low temperature requirements of the system [20]. Additionally, while less syngas cooling is proposed as an advantage of H_2 selective membranes, the syngas is available at different temperatures and pressures at different points within the gasification treatment process. By choosing a high temperature feed stream ideal for the high temperature operation of the H_2 selective membrane, additional cooling is needed later on in the CO_2 compression.

The alternative to a hydrogen-selective membrane is to use a CO_2 selective membrane. Han and Ho examined CO_2 selective facilitated transport membranes for IGCC power plant carbon capture. They used a more recent version of the same baseline NETL report as Merkel et. al, with General Electric's (GE) radiant gasifier as the base case[21].

Several benefits were proposed by Han and Ho of using facilitated transport CO_2-selective membrane over the traditional approach of using polymeric membranes in the CO_2/H_2 separation. First, the higher selectivity possible with facilitated transport membranes means that membranes alone could provide the separation needed, without the need for distillation equipment. Additional advantages lie in that the H_2 pressure is maintained for combustion. Since the syngas feed contains a greater quantity of H_2 than CO_2, using a CO_2-selective membrane means that less gas ultimately needs to be recompressed.

While similar to the Merkel study in scope and purpose, there are several key differences between the two analyses. First, the membrane costs used in the two analyses are quite different ($500 in Merkel vs. $59 per square meter in Han), and different approaches are used in costing the process equipment. Han et al. uses a module-based costing approach, while Merkel et. Al. uses a linear-cost model for capital equipment costs. While Han uses a 4-year membrane lifetime as opposed to the 5-year lifetime proposed by Merkel, the costs still remain quite different. Additionally, Han estimates the membrane replacement cost at $1.25 per square ft ($13.45 per sq meter), whereas the Merkel paper's replacement costs are not indicated to be any different than the original instillation cost (although they are not specified).

Han and Ho describe the costs of H_2S removal for a single stage Selexol process at $198/MW_e$, while in the Merkel report H_2S is co-injected with CO_2. Additionally, Han explicitly calls out the costs of mercury and sulfur (Claus process) at $64/MW_e$ and $6/MW_e$ respectively.

Membranes are versatile and can be used with different types of processes. As demonstrated by Merkel et al., can be combined with cryogenic distillation equipment. Scholes et. al demonstrated that membranes could be combined with adsorption to provide a higher purity CO_2 stream compared to adsorption alone [22]. The authors found that two stages with adsorption provided acceptable CO_2 capture. Janakiram et al. demonstrated that different membrane types can also be used together to lower the overall separation energy than would be achievable by either membrane type alone [23].

Membrane modules can be in several difference types, including plate-and-frame, spiral-wound, tubular, and hollow-fiber. Of these membranes, hollow-fiber have the highest surface area per unit volume, providing the most compact footprint of membrane technologies [4]. The surface area-to-volume ratio depends on the pore diameter, and ratios between 1,500 to 10,00 m^2/m^3 are common.

1.2 Motivation

The aim of this thesis is to provide a comprehensive look into the development of a process configuration, operating and capital costs, and performance of facilitated transport membranes developed at NTNU in an application that is well-defined and documented. Another aim of this thesis is to provide a comparison of the technology developed at NTNU to other available technologies.

The hollow-fiber facilitated transport membranes used for this study have several key advantages that could prove useful in carbon capture applications. Their high packing density results in a low footprint. Minimal solvent usage provides an environmental benefit. Several other studies have indicated that membrane-based technologies can be competitive with existing absorption-based CO_2 capture technologies in IGCC plants [17,

20, 21]. However, within these studies there are many additional variables beyond the membrane performance that are not analyzed to understand their effect on the process. Additionally, the financial models used in these studies are often simple, using a linear model for equipment that does not scale linearly in cost. Few estimations using facilitated transport membranes in IGCC power plants in particular have been completed, and none of those have presented the results in terms of levelized cost of electricity, a key metric to measure cost relative to a plant's expected operating lifetime. The IGCC application is especially important as it involves the simultaneous purification of two gases of high importance today: carbon dioxide and hydrogen. Beyond power, coal gasification with carbon capture has the potential to produce a wide variety of useful other chemicals, including hydrogen, which is viewed as an important energy carrier for industries such as transportation [24]] [25]. Therefore, it is worthwhile to explore the financial viability of novel membranes developed at NTNU.

As the need for sustainable energy becomes increasingly apparent in today's political climate, making available energy sources as sustainable as possible gains importance. While not the cleanest fuel source, coal forms a portion of the energy supply in many large countries throughout the world, and represents approximately 70% of proven fossil fuel reserves [26]. IGCC power plants also have higher efficiencies and reduced emissions of particulates and other pollutants compared to traditional pulverized coal power plants, creating a lesser impact to human health.

By calculating the costs associated with NTNU's facilitated transport membranes in an IGCC power application, baseline costs with the best technology today can be established. Comparisons can be made to other competing technologies, such as adsorption. As advances to membranes are made in the future, progress can be measured in financial metrics compared to the baseline estimations from today's membranes.

1.3   Scope

The scope of this work includes a techno-economic analysis of facilitated transport membranes developed by the team at NTNU. The application for the project is an integrated-gasification combined cycle power plant, with NETL's report on Case 5B chosen as the reference case for applicable stream data and baseline technology comparison [27]. The flowsheet is developed for the membrane separation and CO_2 compression using a combination of Aspen HYSYS, literature costing methodology, and internal membrane simulation software (Chembrane). This project only analyzes the process and cost CO_2 separation stage with conditions that are similar to the existing process.

After this introduction, the thesis is divided into several parts. First, theory involving membranes and carbon capture is explored. Next, the methods used in the process flowsheet development and cost estimates are presented. Then, the results of the process and financial modeling are discussed. Finally, the report is concluded, and recommendations are made for further work.

2 Theory

This section discusses background theory relevant to the topics contained within this report. First, carbon capture is discussed. Next, background on gasification is presented. Lastly, membranes are explored in more detail, with a focus on facilitated transport membranes.

2.1 Carbon Capture

Several different key technologies exist in the CO_2 separation space. Adsorption, absorption, and membranes are three technologies with active, ongoing research. Membranes in particular have distinct advantages, including compact footprint, ease of operation, and competitive costs.

While carbon could be captured alongside other gases, a separation occurs in carbon capture to remove other components. Typically, this is done for practical reasons. This has advantages from an energy standpoint, as inert impurities cause an increase in energy consumption if the gas is later recompressed. The final CO_2 product likely has specifications that require the removal of other gases [4].

2.1.1 Post-Combustion CO_2 Separation

Post combustion CO_2 separation involves separation of carbon dioxide from the other components in flue gas, after combustion [4]. There are several different primary technologies for this approach, with additional variations in each technology in process design, materials used, cost, and performance. As a whole, the main disadvantage to post-combustion CO_2 separation is the large amount of nitrogen that is typically present in flue gas streams. The large amount of nitrogen leads to a lower concentration of CO_2. Combined, these factors are disadvantages of common technologies as they require larger equipment to achieve separation

2.1.2 Pre-Combustion CO_2 Separation Technologies

In pre-combustion carbon capture, carbon is removed from the fuel source prior to combustion. Pre-combustion capture typically results in a lower energy penalty compared to other methods of capture [28]. Pre-combustion is advantageous to membranes as the syngas has high partial pressures of CO_2, due to the combined higher pressure and concentration of CO_2 in the syngas compared to in flue gas.

2.2 Gasification Theory

Coal in its natural state is in a solid form. However, gaseous fuels are often easier to transport, process, and combust. Therefore, gasification can be used to create a syngas from coal, which can more easily processed.

Gasification can be described as a series of reactions that occur within a gasifier and a water gas shift reactor. First, the coal is partially combusted to the principal products of CO and CO_2 [26]. These two reactions are exothermic, resulting in the release of energy that is needed for the further steps. Then, the carbon in the coal is gasified into CO and H_2 in two endothermic reactions listed in Table 2-1. Gasifiers are designed in a

variety of reactor types, dependent upon the supplier. Fluidized bed, moving bed, and entrained flow gasifiers are all commercially available [6].

As CO is not a desired final product, further processing takes place in the water-gas shift reactor, where the CO is reacted with steam to produce an outlet stream with the desired products of CO_2 and H_2. The water gas shift reactor is typically a fixed-bed reactor, with additional cooling to control the exothermic water-gas shift reaction [6]. The catalyst chosen is depending on the likelihood of poisoning from trace elements, namely H_2S [25]. However, CO remains a significant impurity, comprising approximately 1% of the shifted syngas.

Table 2-1: Gasification reactions [6] [26]

Reaction	Chemical Formula	ΔH (kJ/mol)
Gasification with O_2	$C + 1/2\ O_2 \rightarrow CO$	-126
Combustion with O_2	$C + O_2 \rightarrow CO_2$	-406
Gasification with CO_2	$C + CO_2 \rightarrow 2\ CO$	78
Gasification with Steam	$C + H_2O \rightarrow CO + H_2$	119
Water Gas Shift	$CO + H_2O \rightarrow CO_2 + H_2$	-41

The gasification process converts a high percentage of the solid fuel into gaseous form, as over 99% of the carbon exits the gasification process in the product stream [29]. The remaining carbon exits as solid waste.

2.3 Mass Transport in Membranes

Diffusion forms the basis of membrane mass transport [15]. In diffusion, the molecules in a solution randomly move, and eventually there is a net transfer of molecules from the high concentration area to the lower concentration area. Fick's law of diffusion, first proved experimentally in 1855, can be written as

$$J_i = -D_i \frac{dc_i}{dx}$$

Equation 2-1

J_i describes the flux of component *i* through the membrane. As the negative sign suggests, the concentration decreases as molecules move from higher concentrations to lower concentrations. However, the average concentration throughout all of the volume stays the same. In practice, membranes are at the interface of two different concentrations. The ability of membranes to selectively allow certain molecules to pass through more quickly than others is a key part of their utility.

The change in concentration with regards to both time and distance can be described in Fick's second law:

$$\frac{dc}{dt} = -D \frac{\partial^2 c}{\partial x^2}$$

Equation 2-2

20

Together, Fick's laws help describe the solution diffusion mechanism. Many different physical phenomena can create a gradient. These can be differences in concentration, pressure, electrical potential, or temperature.

Principally, there are two different models that propose how molecules flow through a membrane. The first is the pore-flow model, where pressure transports the permeate through pores [15]. The basis for separation in this model is size, where larger particles or molecules cannot pass through the pores. This model was the most popular explanation for membrane separation up until the 1940's.

2.3.1 Solution-Diffusion Model

The solution-diffusion mechanism was first observed by Thomas Graham in the 19th century. He proposed that gases dissolved into the rubber, and then diffuses through the membrane due to the concentration gradient within the membrane [30]. Today, this is understood as the dominant model for mass transfer through a membrane.

Figure 2-1 indicates the schematic of a typical dense membrane. Each layer within the membrane has a specific and vital function [31]. The porous support provides a strong, cheap structure that the rest of the membrane is built upon. The gutter layer serves as a barrier, to prevent intrusion of the selective layer from plugging open pores. The selective layer serves at the main separation interface, selectively allowing the desired molecule through, ideally at a higher permeance. The protective layer serves to prevent damage to the selective layer, which could hinder membrane performance if holes or imperfections are created in the selective layer during membrane module fabrication.
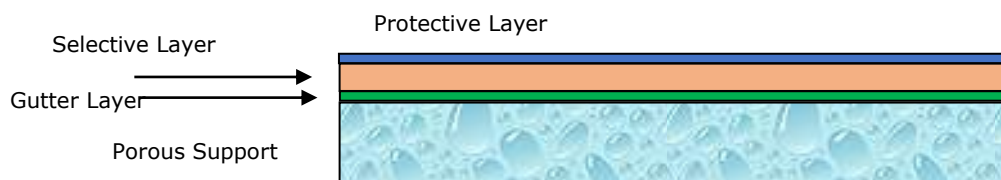
Figure 2-1: Schematic of a dense composite membrane. Adapted from [31]

In the solution-diffusion mechanism, the gas molecules diffuse through the bulk.

2.3.2 Pore Flow Model

The pore flow model, describes that mass transfer through a membrane can be described as flow through a series of pores through the membrane volume. The Hagen-Poiseuille equation, describing incompressible flow, can be used to model flow through a constant, cylindrical void [10].

$$J = \frac{\varepsilon \, r^2}{8 \, \eta \, \tau} \frac{\Delta P}{\Delta x}$$

Equation 2-3

Where J si the solvent flux, ε is the surface porosity, τ is the pore tortuosity, r is the pore radius, η is the solvent viscosity and $\frac{\Delta P}{\Delta x}$ is the driving force across the membrane. While this could model membranes made up a series of pores quite well, in practice most

membranes are not of this composition. Compared to the solution-diffusion mechanism where the pressure is assumed to be constant across the membrane with a concentration gradient determining the chemical potential, in the pore-flow model the pressure drop through the membrane governs the driving force [32].

In membranes, it's quite common to have multiple regions with different properties. An assymetric membrane will have various regions of the same material, each with different properties.

2.3.3 Facilitated Transport

Facilitated transport membranes offer a potential pathway to allow for select molecules to permeate more quickly through a membrane than other molecules. In the case of CO_2, polar amine groups can be utilized to reversibly bind to the carbon dioxide. Either fixed or mobile carriers can promote facilitated transport [33]. Typically, these interactions occur either at depressed temperatures or close to ambient conditions. Other polar molecules, such as H_2S and H_2O, also permeate more quickly based on this interaction, whereas non-polar molecules, such as N_2 and H_2, permeate more slowly. The transport of CO_2 can be enhanced by water-induced interactions and swelling within the membrane [34]. Therefore, optimal performance of PVA membranes can be assumed to occur close to 100% relative humidity. An illustration of facilitated transport within a membrane can be seen in Figure 2-2.

By actively transporting CO_2, facilitated transport membranes have key advantages over traditional polymeric materials that rely on the solution diffusion mechanism alone. The equation for the permeate flux has an addition term, representing the active transport of the molecule in addition to the solution-diffusion mechanism [13].

$$J_A = \frac{D_A}{l}(C_{A,0} - C_{A,1}) + \frac{D_{AC}}{l}(C_{AC,0} - C_{AC,1})$$

Equation 2-4

The movement of the CO_2 is facilitated through a complexation between water, the amine group, and CO_2. By adding another transport mechanism besides the traditional solution diffusion mechanism, there is another driving force to transport the CO_2 molecule through the membrane. In theory, this has the advantage of allowing for CO_2 to be transported across the membrane even against the concentration gradient if transport is coupled with another species, typically water, that is transported normally. As part of this mechanism, water is essential.

The mass transfer through the membrane can either be thought of being diffusion limited or reaction limited [35]. When the complexation reaction is very fast, mass transfer is determined by the rate of diffusion into the membrane. On the other hand, when the complexation reaction is slow, the rate of mass transfer is instead determined by the reaction rate. Between these two limits, both reaction and diffusion rates contribute significantly to the mass transfer. In biology, active transport systems exist within the cells to transport molecules against the concentration gradient.

 An additional benefit of the positive interaction of water in an IGCC power plant is that it eliminates the need for removal of water within the shifted syngas, which is fully saturated with water vapor. The flowsheet of the IGCC power plant can be found in Appendix 2.

Within facilitated transport membranes, operating pressure plays an important role. Several studies have found the above certain partial pressures, the effectiveness of

facilitated transport membranes compared to traditional polymer membranes is reduced [15] [36].

Two mechanisms are proposed for the facilitated movement of solutes in fixed site carrier membranes [15]. The first, proposed by Cussler, Aris, and Bhown, is the "Tarzan Swing" mechanism, in which complexing sites need to be close enough to complete a "handoff" from one agent to the next. This type of mechanism can be seen in Figure 2-2. This means that if the distance between complexing agents is too far, the solute flux would drop. Another proposal, presented by Noble, is that the solutes travel along the polymer chain to reach another complexing agent. At higher relative humidity, a swelling effect occurs, and aqueous domains occur in between the hydrophilic chains of polymer promote mass transfer if the polymer is sufficiently crosslinked for mechanical strength [37].
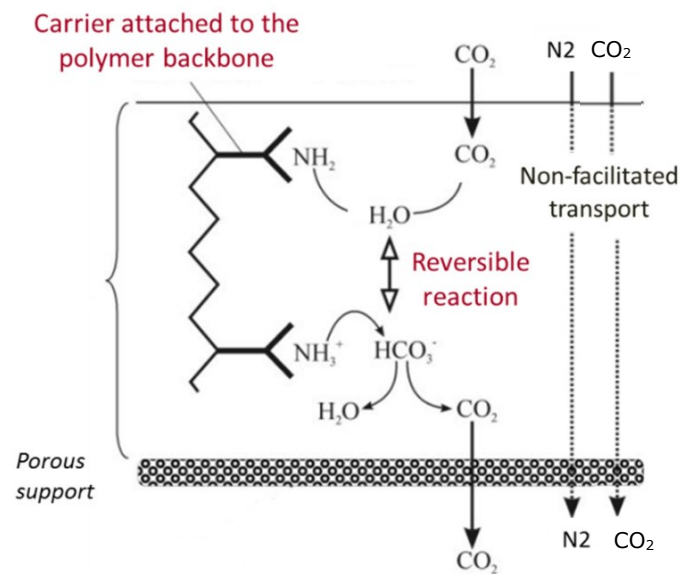
Figure 2-2: Depiction of facilitated transport mechanism. Adapted from [38] [39] [40]

Several reactions are important for the reverse reactions associated with facilitated transport, which are reversible and involve the formation of a carbonate ion [15].

$$CO_2 + H_2O \leftrightarrow H^+ + HCO_3^-$$

Equation 2-5

$$CO_2 + OH^- \leftrightarrow HCO_3^-$$

Equation 2-6

$$HCO_3^- \leftrightarrow H^+ + CO_3^{2-}$$

Equation 2-7

$$H^+ + OH^- \leftrightarrow H_2O$$
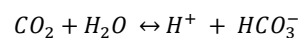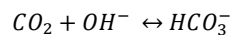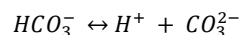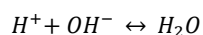
Equation 2-8

The reactions listed above do not occur at the same speed. Reactions 2-5 and 2-6 occur very slowly, while 2-7 and 2-8 occur very quickly. The effect of water in the membrane is important.

Facilitated transport membranes help accelerate transport through a membrane, up until a certain point. That point is called the carrier saturation limit [41]. Upon increasing the driving force further beyond that threshold, facilitated transport adds no additional flux beyond that of solution-diffusion. However, at very low driving forces, when flux via diffusion is limited, facilitated transport mechanisms contribute much more significantly to the flux through a membrane.

Several advantages lie with utilizing facilitated transport-based membrane separation over other separation methods [41]. First, the membranes can achieve separations more easily than many other methods at low driving forces. Having facilitated transport gives these membranes advantages over other membranes at lower driving forces. The solvent utilized is also significantly less compared to liquid solvent-based separation methods, yielding less risk of spills or environmental release, and less cost associated with maintain the liquid solvent. Because of the smaller amount of chemical reagent used, more complex chemistries can be utilized. Membranes can also be utilized in small footprint applications, and then adapted to a larger scale with less difficulty than other separation methods.

Use of facilitated transport membrane is not without difficulties. Challenges lie in the stability of the membrane carrier agent, along with the potential for impurities in gas streams to poison the carrier sites [15]. Additionally, facilitated transport membranes have been proven in pilot studies to be effective in operation at temperatures up to 100 °C [36].

2.4   Membrane Performance

The materials that comprise a membrane determine its properties. In polymeric membrane, the glass transition temperature, denoted T_g, plays an important role. Below this temperature, the polymer is in a glassy state. Above this temperature, the polymer is considered to be rubbery. When below the glass transition temperature, polymers can be either crystalline or amorphous. In general, crystalline polymers usually have lower gas solubilities. Rubbery polymers usually have higher permeabilities for gases, and therefore are often more desirable for gas separation applications.

Membranes can also be constructed to impact their performance. Asymmetric membranes rely on varying regions within the membrane to have different properties [31]. In composite membranes multiple materials comprise the membrane. Typically, a composite membrane contains a porous support to provide mechanical strength, and a thin selective layer, with a buffer in between to prevent the coating process from plugging membrane pores. By having the ability to control the selective layer in a composite membrane, the properties and performance of a membrane can be enhanced for the desired separation [42]. For each application, a different selectivity or permeances may be advantageous. High selectivity or permeance are not without their disadvantageous. As the Robeson plot indicates, the highest selectivity membranes have relatively low permeance, and vice-versa [43]. This is because selective membranes are typically limited by diffusion, already a slow process. For many applications, having high selectivity but less permeance is a large drawback as either the process pressure or membrane area would need to be increased.

As membrane technology has developed, so to have the capability of membrane materials. The seminal article *The Upper Bound*, published in 1991, graphically indicates the best performance of membrane materials at the time of its publication. In the

following years, advances in membrane technology meant that the upper bound had to be revisited, as the prior limits to selectivity and permeance had been surpassed [43]. As new materials and methods of fabricating membranes are established, the capabilities of membranes have been continually improved [44].

Membranes can be fabricated from a variety of materials [10]. The properties of membranes can be analyzed with in several key parameters. Equations relating to this are discussed, along with their importance in different membrane applications.

The first parameter is permeability, which is defined by the equation 2-9[45].

$$P_i = D_i * S_i = \frac{l * J_i}{A *}$$

Where P_i is the permeability, D_i is the diffusivity of component "i", S_i is the solubility, q_i is the flux of "i", A is the surface area of the membrane, and Δp_i is the difference in partial pressure of component "i" across the membrane that has thickness "l".

In most membrane systems, multiple solutes are present. Some of these solutes are desired to be transported through the membrane into the permeate, while others are desired to remain in the retentate. The rate of relative transport through the membrane determines the selectivity. It can be described using

$$\alpha_{ij} = \left(\frac{D_i}{D_j}\right)\left(\frac{S_i}{S_j}\right)$$

The two determine factors in selectivity are D, the diffusion coefficient, and S, the sorption coefficient. Some very selective membranes, such as some that are used in reverse osmosis applications, can achieve selectivity ratios of over 10,000 [15].

3 Method

This chapter discusses the methods used in the developement of this report. First, background is presented on the methods used in the base case used as part of this project. Next, the development of the flowsheet and process configurations are discussed. Then, costing of equipment and operational expenses are discussed. Finally, the techno-environmental metrics used to measure the cost-effectiveness of carbon capture are outlined.

3.1 Base Case Background

The United States NETL (National Energy Technology Laboratory) has released several reports estimating cost for electricity generation from coal and natural gas sources [27]. Thirteen configurations of power plants are provided with detailed cost and process information. These reference cases are extremely useful, as power plants of the same size and technology can be compared with different metrics. Having set data, such as material streams, plant sizes allow for some baseline assumptions to be established consistently so that further reports based off of these initial datasets can be more streamlined and use similar data.

Three gasification system designs were considered for inclusion as the base case and are displayed in Table 3-1. These include designs by Shell, CB&I, and GE. Each of these three scenarios also has an equivalent scenario with 90% of the CO_2 captured using a Selexol process. Variations in design of these plants affect their efficiencies, capacities, and suitability for carbon capture.

Table 3-1: Cost parameters summary of potential IGCC power plant designs

Brand →	Shell		E-Gas FSQ		GE	
Parameter	w/o CCS	w/ CCS	w/o CCS	w/ CCS	wo/ CCS	w/ CCS
Total Plant Cost ($/kWhr)	3,824	6,209	3,395	5,177	3,822	5,240
LCOE including T&S, $/Mwhr	105.8	175.0	97.5	143.1	107.9	144.2
Portion Capital Costs $/MWhr	54.5	88.9	48.4	74.4	54.7	75.2
Portion operating costs ($/mWhr)	51.1	86.1	49.1	68.7	53.2	77.1
Breakeven CO_2 sales price, $/ton	-	119.4	-	96	-	98.1
Breakeven CO_2 emissions penalty	-	162.7	-	126.9	-	128.3

These costs differences can be explained by several factors, including the type of coal feed, the gasifier efficiency, and type of technology used. Of particular importance for the carbon capture is the feed of coal. If coal is fed in slurry form, the additional water is beneficial for the water-gas shift reactor used in the carbon capture cases. Additionally, different technologies are utilized for separation of the H_2S and particulate matter, and treatment of the process water between the different cases.

Several assumptions are made within the NETL report that are continued in this financial analysis to serve as a comparison point [27]. First, the plant is assumed to be located in the midwestern United States, and all costs are estimated in 2018 United States Dollars (USD, or $). For purposes of comparison and consistency, financial data in this report is also presented in 2018 USD. For IGCC power plants, the capacity factor is assumed to be 80%. The availability is assumed to be interchangeable with the capacity factor, i.e., the plant is producing nameplate capacity for 7,008 hours per year. The capacity factor is expected to remain constant over the plant's expected 30-year life.

The power plants of interest for the purpose of this report are described in case B5A, which is an IGCC power plant without carbon capture using a GE gasifier design, and 5B5, which uses the same technology with the addition of carbon capture [27]. Both plants use an 1800 psig (124 bar) steam cycle operated at 1000°F (538°C). The plant uses 2 advanced GE F-class turbines, and the gasifier is a radiant gasifier. H_2S separation is accomplished using the Selexol process, and sulfur is removed using the Claus process. Particulate matter (PM) is removed using a quench, water scrubber, and acid gas removal (AGR) adsorber. Process water is treated using vacuum flash, brine concentration, and crystallization. Case B5B uses the same process technologies, with the addition of a water-gas shift reactor to reduce the amount of CO in the syngas, and a two-stage adsorption-based Selexol process to remove CO_2 from the Syngas. The plant size is determined by commercially available turbine sizes. It is worth noting that the plant includes some environmental pollution controls to meet the limits set by the 2013 update of the US regulation on New Source Performance Standards (NSPS) for air pollutants that include nitrogen oxides (NO_x), sulfur dioxide (SO_2), particulate matter (PM), mercury (Hg), and hydrochloric acid (HCl), meaning that the plant meets national environmental regulations around these pollutants.

For the data presented with the baseline Selexol process, case B5B-Q, which involves a quench-only gasifier, provided the lowest levelized cost of electricity. However, this report focuses on case 5B, which is a radiant-quench gasifier, for several reasons. First, case 5B has a higher plant efficiency, which at a 90% capture rate results in less CO_2 emissions per ton of fuel used. Since the goal is carbon capture, this an important consideration in the choice of process equipment. The GE process selected for the base case is also the most widely used in power generation applications today and is competitive on costs to the other scenarios. Additionally, previous literature studies focus on the B5B case, so focusing on B5B provides a more accurate point of comparison with respect to costs and process equipment sizes [20, 21]. With the costs, it is important to understand that there is uncertainty in the estimates provided. The NETL estimates there to be a -25/+50% uncertainty in the actual costs associated with IGCC projects [27]. This is larger than other types of power plants, such as pulverized coal and natural gas combined cycle, as less IGCC plants have been built. If IGCC technology continues to be built and matures, costs will likely be reduced in uncertainty. As noted in the report, project costs are site, project, and time specific. Costs depend on local geographical conditions, input costs, and project strategy.

The NETL report also makes assumptions based on the price of coal that are embedded into the costs used as a base case for this work. Coal is assumed to cost $2.11/GJ on a levelized basis in 2018 values. Further key estimated costs are presented in Table 3-2.

Table 3-2: Key cost assumptions of process inputs [27] [27] [46]

Item	Assumed Cost	Per unit
Coal	$2.11	GJ
Carbon Transport and Storage	$10	Metric ton
Electricity	$108	MWhr
Cooling Water	$2	GJ

Case 5B estimates costing including carbon capture. The transport and storage costs are assumed based on a 62 km pipeline that transports the CO_2 into a deep saline formation. The transport and storage costs are estimated at $10 per metric ton, which are utilized as the cost for transport and storage in this report as well.

Costs in the future are likely to change, especially for items such as fuel, labor, and environmental regulations. However, by providing a consistent estimation basis, alternative technologies can be compared without vast differences in assumptions.

Several alternatives of costing methodology are also available. Different methodologies and equipment assumptions can lead to significantly different costs associated with carbon capture projects [47]. The methodology chosen is to use the module based approach, which can be useful in determining the non-linear relationship between equipment size and purchased cost [46].

3.2   IGCC Process Description

This section highlights key aspects of the power generation process. A process flowsheet of the IGCC power plant can be found in Appendix 2. The following briefly describes at a high level the underlying process assumptions for the IGCC power plant, which determines the properties of the syngas delivered to the membrane separation units.

The air separation unit used is a cryogenic air separation unit. The air enters the unit where it is filtered, compressed, and then cooled with chilled water. Air is discharged out of the ASU at a pressure of 1.6 MPa. The unit consumes 420 kWh per ton of O_2 produced, contributing a significant portion of the plant energy usage. Air is delivered at a quality of 95%. Nitrogen is also produced, with an oxygen content below 2%. [27]

The gasifier helps drive more complete conversion of the syngas into the desired components of H_2 (for combustion) and CO_2 (for capture). The water-gas shift reactors uses four reactors across two parallel paths to achieve a 95% conversion of CO. [27].

Mercury can be removed from IGCC plants more easily than in traditional coal power plants. The volume of syngas produced is much smaller than the flue gas produced during combustion with air. As the merucry is contained within the syngas, it is easier to treat the smaller volume of syngas prior to combustion. Data from the NETL report on based on operational data from a syngas facility baed in Kingsport, Tennessee, US. The technology utilized at the location is a packed carbon bed vessel. The carbon bed is

located before the acid gas removal process to optimize the termperature of the syngas for Hg removal. There is one cabon bed per gasifier, for a total of four carbon beds. Once spent, the carbon beds are considered hazardous waste due to their high mercury content. [27].

Sulfur, when combusted, has the potential to form hazardous emissions. Therefore, sulfur is removed from the syngas prior to combustion. Several competing technologies are available for sulfur removal. The first step in removing sulfur from the syngas is to ensure it is an easily removable form. To eliminate COS, the hydrolysis reaction is utilized. Typically conversion of COS for this reaction are around 95%,which result in most of the sulfur in more easily removable H_2S [27].

$$COS + H_2O \Leftrightarrow CO_S + H_S S \qquad \textbf{Equation 3-1}$$

The H_2S can then be removed by a number of solvent based absorbent processes. More than 30 different technologies are in commerical use across a variety of industries. Several proceess are cosnidred in the different scenarios for the baseline technology. However, excusively the selexol process is utilized for scenarios with carbon capture.

Some disadvantages to the Selexol process include the large equipment footprint and energy costs associated with it. Additionally, some equipment requires stainless steel, further adding to the cost.

Syngas requirements are based on the specifications presented in the NETL report [27]. In particular, the pressure, (3.1 Mpa) and LHV (3 kJ/mol) are the two main considerations for the final syngas product fed for power generation.

The CO_2 product is compressed with multistage compression with intercooling for transport via pipeline. The final CO_2 product has a pressure of 152 bar and a temperature of 30°C.

3.3 Process Simulation

The process utilized Aspen HYSYS version 11 software integrated with Chembrane version 7.0, an in-house program used for calculations on the membrane units within the system [48]. The software has the ability to model different flow patterns. The highest packing densities can be found in hollow fiber membranes, and therefore in this case the flow was assumed to be counter-current [45]. Chembrane uses a 4th order Runge-Kutta approach to calculate the feed side molar flows and compositions. Then, the permeate compositions and flows are iteratively calculated until the solution is within an acceptable range. No pressure or temperature drop occurred on the retentate side of the membrane.

The feed streams are taken from the NETL baseline report [27]. Stream 25 is chosen as the desired feed point for the syngas separation to occur. At this point, the syngas has already undergone the water-gas shift reaction and been scrubbed with ammonia . Mercury has been removed from the gas stream. Most importantly, the initial stream temperature of 36°C falls within in the operating range of facilitated transport membranes and closely matches the experimental data for the membrane. The feed pressure of 42.1 bar provides a high degree of driving force across the membrane. For purposes of the simulation, the gas stream is considered to be a mixture of CO_2, H_2, H_2O, N_2, and CO. Other, trace elements such as CH_4 and Ar are not included in the simulation. The feed stream is assumed to be free of solids.

The feed is assumed to be split into two streams for purposes of handling and equipment sizing. While this doubles the number of process equipment used, the equipment becomes more manageable to produce and all within acceptable sizing parameters. This is similar to the design of the combustion system, which already uses two parallel turbines to generated power [27]. The two primary products of the simulation are the syngas, used for combustion, and the CO_2 stream, which is compressed for transport or storage.

As indicated in the baseline document, the syngas is mostly processed in two identical trains [27]. The splitting of the syngas into two streams allows for size limitations on equipment to be accounted for. As the trains are identical, only one train is simulated in HYSYS and the equipment, capital, and operating costs are all doubled to account for the entire process.

Table 3-3: Component gas membrane performance used in the simulation [49], [50]

Gas	CO_2 selectivity	Permeance ($\frac{mol}{m^2 \times kPa \times hr}$)
Hydrogen*	44	2.77E-03
H2O	1	1.22E-01
Nitrogen	100	1.22E-03
CO2	1	1.22E-01
H2S	1	1.22E-01
CO	44	2.77E-03

*Note – He is used for permeance calculations.

The simulation is based on experimental laboratory data presented in Table 3-3 which recorded at NTNU for the selectivity and permeance of CO_2 and H_2 [49]. Estimates for selectivity with respect to N_2 is taken to be within the range of similar documented membranes [50]. H_2S and H_2O are all estimated to have the same permeance as CO_2 as they are all small, polar molecules.

Other assumptions are made for the purposes of the simulation. Compressors and expanders are assumed to have an efficiency of 85%. Heat exchangers, membranes, and process piping, and vessels are assumed to have no pressure drop across the equipment.

The performance criteria for the system are described in Chapter 4, as well as Appendix 16. These are selected loosely off of the Selexol baseline results. It is important to note that slight variations in performance may have an impact in cost that are outside the scope of this report.

Two membrane stages are used in this model of the membrane process. The syngas enters the membrane system and a temperature of 36°C and a pressure of 42.1 bar. The syngas is passed to the membrane, with the retentate from the first membrane stage sent directly to combustion. The 1st stage retentate is then passed to a second membrane stage, either with or without recompression. The second membrane stage provides further separation. The retentate of this stream is either sent back in a recycle or sent directly to combustion depending on the process configuration. The retentate of the second stage is compressed in an 8-stage compression train with intercooling.

Several variables were examined in the course of this simulation and their effect on membrane performance. The variables tested are in Table 3-4. All stream names refer to the process flowsheets found in Appendix 3, Appendix 4, and Appendix 5.

Table 3-4: Membrane Parameters altered in simulation.

Variable	Description
$R_{CO2,1}$	Stage 1 recovery
F_5	Stage 1 sweep stream flowrate
$X_{CO2,15}$	Second stage retentate CO_2 mole fraction
P_9	Stream 9 Pressure
P_{10}	Stream 10 pressure
P_{16}	Stream 16 pressure

Two alternative membrane configurations are used in the process, as shown in Figure 3-1. Configuration A included a recycle stream after the second membrane stream, while in configuration B the second stage retentate is sent with the first stage retentate to combustion. The two configurations are analyzed with the same parameters, with the addition of $X_{CO2,15}$ in configuration B.
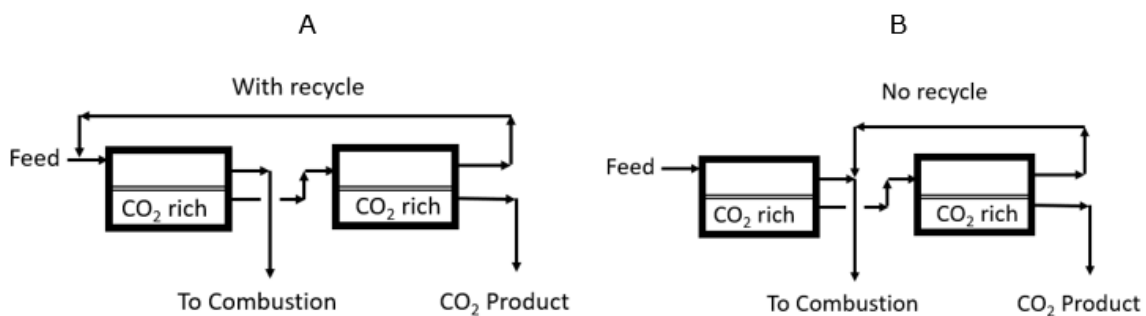
Figure 3-1: Process Configurations Analyzed

In addition to the high level overview presented in Figure 3-1, a more detailed view of the process system can be found in Appendix 13 and Appendix 14. These diagrams, based on a similar presentation of a different system by Yuan, map the variables tested in the simulation with respect to a basic process block diagram [51]. Key assumptions, based either on the baseline documents or laboratory data, are marked in green rectangles. Design variables, which are tested as part of this analysis, are marked in blue squares. Dependent variables, which are monitored as part of the analysis as they are key performance targets, are marked with orange triangles. While there are other variables that could be tested, the variables selected were chosen based on their need to be specified within the process, and the speculation of potential impact to the process. The examined cases used the parameters presented in Table 3-5.

Table 3-5: Range of parameters tested in the simulation

Parameter	Description	Units	Min	Max	Step Size
F_5	Flow of sweep (H$_2$O), stage 1	Tons/hr	0	100	10
P_{16}	Recycle recompression pressure	Bar	31	42	2.75
$X_{CO2,15}$	Mole fraction CO$_2$, recycle	Mole %	0.025	0.125	.025
P_9	Stage 1 permeate pressure	Bar	1	15	1
P_{10}	Interstage recompression pressure	Bar	4	16	1
$R_{CO2,1}$	Stage 1 CO$_2$ recovery	%	80	95	1

*Only in configuration B. For configuration A, the CO$_2$ concentration was fixed to .4088 (same as feed composition)

3.4 Capital Costing

3.4.1 Baseline Cost Data

Basleline cost data for the construction of a power plant is taken from calculated from case B5A costs in the NETL report on power generation [27].

3.4.2 Process Equipment

To calculate the capital costs associated with the separation equipment, a module-based costing approach was used [46]. First, the purchased equipment costs were calculated using the factors as described for the appropriate equipment type. The sizing was based on cost correlations with the relevant equipment sizing factor, which is power used for compressors and area for heat exchangers. A heat transfer coefficient of 30W/m^{2}K and a log-mean temperature difference of 10 K were assumed for all heat exchangers. The area of the heat exchanger is calculated using equation:

$$A = \frac{Q}{U \Delta T_{LM}}$$

Equation 3-2

Where Q is the duty, U is the heat transfer coefficient, and ΔT_{LM} is the log mean temperature difference. For the purpose of this simulation, ΔT_{LM} is assumed to be constant at 15K and the overall heat transfer coefficient, U, is assumed to be 200 W/m^{2}k.

After finding the key sizing parameters, the following equations was use to calculated the purchase cost of compressors and heat exchangers [46].

$$log_{10} C_p^0 = K_1 + K_2 log_{10}(X) + K_3 [log_{10}(X)]^2$$

Equation 3-3

Where X is the sizing parameter of the equipment, as seen in Table 3-6.

Table 3-6: Capital costing parameters for key process equipment

Description	Parameter and unit
Heat Exchangers	Area, m^2
Compressors	Fluid Power, kW
Process Vessels	Volume, m^3
Membranes	Area, m^2

Heat exchangers are calculated with the sizing parameters in Table 3-7. A fixed tube heat exchanger was chosen as the desired type due to the large areas and high-pressure range available for this type.

Table 3-7: Heat Exchanger Sizing Parameters

Heat Exchanger Type	K_1	K_2	K_3	$A_{min(m2)}$	$A_{max(m2)}$
Fixed tube, sheet, or U tube	4.3247	-0.303	0.1634	10	1000

The coefficients used for compressors and drives in equation 3-3 can be seen in Table 3-8 and Table 3-9 respectively.

Table 3-8: Sizing Parameters use for compressor calculations [46]

Compressor Type	K_1	K_2	K_3	F_{BMSS}	$W_{max}(kW)$
Centrifugal	2.2891	1.3604	-0.1027	5.8	3000

It is important to have the drive in addition to the compressor, as the drive converts energy in the form of electricity or stream into mechanical energy to spin the turbine used in compression. Electricity was chosen to be the desired energy source for the drive. While the sizing range for compressors goes up to 3000 kW, the size of the electrical rives electrical drives (motors) are limited to 2600 kW. Therefore, if the simulation indicates that compressors greater than 2600 kW were needed, it was specified that the fewest number of compressors possible would make up that compression stage. It was also assumed that there was one drive needed for every compressor.

Table 3-9: Sizing Parameters use for compressor drives [46]

Electric Drives	K_1	K_2	K_3	F_{BM}	$W_{min}(kW)$	$W_{max}(kW)$
Explosion Proof	2.4604	1.4191	-0.1798	1.5	75	2600

The presence of hydrogen in the syngas presents a potential explosion risk if released [52]. Drives, and other electrical equipment can be designed to prevent the electrical equipment from triggering an explosion n[53]. Even if combustible gas makes its way inside this equipment and reaches an ignition source, the design of the electrical enclosures is such that the flame is extinguished before it can cause a larger ignition outside. The safer design of electrical equipment designed for hazardous locations

reduces a major ignition source for facilities handling flammable gases. The costing parameters for the drives are presented in Table 3-9.

For membranes, the cost of the equipment was calculated using the following equation:

$$C_{membrane} = C_{spef} * A$$

Where A is the membrane area in m^2 and C_{spef} is the specific cost of the membrane in USD/m^2. The membranes this study is modeled off are hollow fiber membranes, which have a higher packing density compared to other membranes. This in turn can lead to a lower membrane cost, as less material is needed per unit of surface area.

Two vessels were located within the process to act as vapor-liquid separation units. It was assumed that these vessels would not change substantially based on the scenarios tested, and therefore were set as a fixed cost based off an initial volume of 66 m^2 and 106m^2 for the two vessels respectively. Costs were obtained using the cap cost calculation software with a designed operating pressure of 12 bar [46].

3.4.3 Additional Costing Parameters

Next, the pressure, and material factors were included to calculate the bare module factor. These factors help account for differences in material and installation costs required with more advanced metallurgy. For equipment in contact with the carbon dioxide streams, stainless steel was assumed to be the material of construction for estimating the material factor. Pressure factors were obtained based on the operating pressure for the separation vessel. After the bare module factors were obtained, the equipment costs were updated to 2018 using the CEPCI value of 603.1 for 2018 [54] using equation

$$C_2 = C_1 * \frac{I_2}{I_1}$$

The year 2018 is chosen as that is the base year for the DOE cost data on the provided energy study [27].

After the bare module costs were calculated, fees of 15% and 3% were added for contingencies and fees respectively. Additionally, 50% of the bare module costs were added to account for auxiliary plant equipment. For membrane equipment, the price of $75/$m^2$ is assumed to be the fully loaded cost of installation, including all auxiliary equipment, fees, and services. The membrane lifetime is assumed to be 5 years.

3.5 Operational Costing

In addition to capital costs, operating costs are associated with additional labor for membranes with carbon capture was estimated at 4 workers at a rate of $35 per hour ($72,800 per year). Electricity costs are based on the U.S. DOE study for the levelized cost of electricity in an IGCC power plant, case 5A, which has a levelized cost of electricity of $107.9 per MWhr [27]. The net generation capacity of the plant without carbon capture is 634 MW. The net generation capacity with carbon capture is the net size of the plant (634 MW) less than energy used in the carbon capture process.

Membrane lifetime is estimated at 5 years and therefore replacements in addition to the additional capital investment will be required at 5 points (5, 10, 15, 20 and 25 years) in the 30-year predicted lifetime. The membrane replacement cost is assumed to

be identical to the initial membrane cost. Operational costs and membrane replacement costs are assumed to remain constant across the project lifetime. Fouling of the heat exchangers and membrane equipment are assumed to be nonexistent. All process equipment is assumed to retain its initial performance capabilities throughout its operational life.

Additional factors related to operational costs are needed to account for other expenses incurred during the operating lifetime of the plant. These include items such as overhead, supervisory, and administrative costs for plant operation; maintenance and repairs to equipment; and other items such as deprecation and insurance. The costs are estimated based on correlated items. Supervisory labor is based on a factor of the direct labor, while taxes are based on the initial capital investment. A complete list of the additional operating cost factors can be found in Table 3-10.

Table 3-10: Operating cost parameters used in calculating the operating costs [46]

Description	Parameter Value
Annual Operating Cost	.18FCIL
Annual Labor Cost Factor	2.76 COL
Annual Utility Cost Factor	1.23 CUT
Grassroots Costs	$0.5C_{BM}$
Total Module Cost	$.15C_{BM}$
Depreciation	10-year, straight line
Tax Rate	25%
Cost of Capital	12%
Land Acquisition Cost	$300,000
Annual Salary	$72,800
Number of operators	4

The annual operating costs comprises aspects such as utilities, labor, overhead, maintenance, and consumables. At a high level, it is more time-effective to calculate costs based on established parameters encountered in previous plant operation to determine the operation costs. The factors used in calculating operating costs are found in Table 3-10. These are based off of the FCIL (Full capital Investment), COL (Cost of labor) and CUT (Cost of utilities).

3.6   Key Carbon Capture Metrics

There are several metrics that can be used in report the costs associated with carbon capture. As each of these metrics has a different meaning and different underlying assumptions, it is important to understand the distinction between different reporting metrics. Within each of these metrics, there are underlying assumptions that have an important impact on the costs reported.

The key quantitative metric for electricity generation in this document is the levelized cost of electricity (LCOE). The levelized cost takes into account that future revenue and costs from electricity generation are discounted with respect to current value. To find the levelized cost of electricity, the following equation is used:

$$0 = \sum_{0}^{n} \frac{LCOE - \text{Discounted Expenses}}{Net\ power\ produced}$$

Equation 3-6

36

where n is the number of years of the project lifetime. The costs included capital and operating costs on a discounted basis. For the simulation, the discount rate used was 12%.

The levelized cost of energy can also be represnted in terms of the percent increase of a reference base power, as indicated in Equation 3-7.

This reduces the impact of having a reference year, as different studies can be compared across years based on their percent LCOE increase [22].

$$\% \ LCOE \ Increase \ = \frac{LCOE_{Membrane} \ - \ LCOE_{no \ capture}}{LCOE_{no \ capture}} * 100\%$$

Equation 3-7

Within the LCOE increase, it is important to understand what costs are included. For the purposes of this analysis to be consistent with other studies, the cost of transport and sequestration of the CO_2 product are not included in the LCOE, while the costs of compression are.

The carbon capture percentage, also termed percent recovery of CO_2, is presented in equation 3-8. This metric refers to the percentage of input carbon to the power plant that is prevented from released into the atmosphere. The calcuclation excludes the 2,791 kg/hr of carbon in the solid slag from the power generation process.

$$CCP \ = (1 - (\frac{Carbon \ emitted \ to \ atmosphere}{Carbon \ in \ - \ carbon \ in \ slag}) * 100\%$$

Equation 3-8

The carbon capture cost, or CCC, was calculated for the plant using the following approach. A membrane lifetime of 5 years was used in the calculation, and no escalation factors or inflation were estimated for capital or operating costs. The power plant was assumed to generate electricity on a consistent basis, regardless of the capture quantity, over a 30-year lifetime, OL. The membrane is expected to have a 5-year lifetime and be replaced five times over the life at a cost of C_{MR}. The cost of carbon capture becomes:

$$CCC \left[\frac{\$}{ton}\right] = \frac{FCI + OL * COM + 5 * C_{MR}}{OL * Capacity_{Gen.}}$$

Equation 3-9

The carbon capture cost is a non-discounted metric, meaning it may not accurately reflect the fact that future revenues from carbon capture have a lesser value to investors than the revenues and capital costs from early in the project.

The cost of CO_2 per ton can be caclculated as the cost of the proces (in this case, electricity generation), which can be calculated as [16]

$$CO_2 \ avoided \ cost \left[\frac{\$}{ton}\right] = \frac{Annualized \ investment \ + \ annual \ OPEX}{Annualized \ quantity \ of \ CO_2 \ avoided}$$

Equation 3-10

The CO_2 avoided cost is also calculated on a non-discounted basis. The distinction between the CO_2 avoided cost and the cost of carbon capture is that the avoided cost takes into account that the extra energy expended by the CO_2 capture process reduces the net power produced by the power plant. The baseline levelized cost of electricity is the \$107/MWhr used in the baseline document case B5A [27].

The breakeven cost of CO_2 sales price is similar to the carbon capture cost, but it is assumed on a discounted basis. This price is the value that would have to be placed on a CO_2 in the product stream for carbon capture to be the same cost as a plant without carbon capture.   The formula to determine the breakeven CO_2 sales price is [27]

$$Breakeven\ CO_2\ sales\ price\ \left[\frac{\$}{ton}\right] = \frac{(LCOE_{CCS} - LCOE_{without\ CCS})}{CO_2\ Captured\ per\ MWhr}$$

Equation 3-11

The breakeven CO_2 sales price is a useful metric if it assumed that there will be a viable market for the CO_2 product stream. This can occur if the project is tied with using the CO_2 for another purpose, such as enhanced oil recovery. An important distinction between this metric and the carbon capture cost is that it assumes a different base cost for the levelized cost of electricity. While the CCC is based off the lowest cost IGCC power plant, the breakeven CO_2 sales price assumes that the comparison point is the lowest levelized cost of electricity using the same fuel source, which in the case of coal is a supercritical CO_2 plant that produces electricity at an LCOE at \$64/MWhr.

The breakeven CO_2 emissions price is the penalty that would have to be placed on emissions in power generation for carbon capture and non-carbon capture to be equal in cost. This is calculated on a discounted basis. This metric is important if a CO_2 market does not fully cover capture costs, but instead emission reduction policy is driven by taxes on carbon emissions. The formula to determine the breakeven CO_2 sales price is [27]

$$Breakeven\ CO_2\ emissions\ penalty\ \left[\frac{\$}{ton}\right] = \frac{(LCOE_{CCS} - LCOE_{without\ CCS})}{CO_2\ avoided\ per\ MWhr}$$

Equation 3-12

The key difference from the sales prices is that this metric takes into account that some of the CO_2 is released into the atmosphere and should be incorporated to the financial metric used to evaluate the project. This also assumes that there is not necessarily a market for a finished CO_2 stream, but instead a penalty on CO_2 emissions.

For purposes of comparison, several cost methods are utilized in this report for a broader applicability and allow for comparison between different other studies. The final state required for the CO_2 will be determined by its end use. For this simulation the CO_2 was assumed to be needed in a liquid state for pipeline transport. Therefore, the CO_2 outlet stream was compressed to a mostly liquid form at 180 bar and -55°C, with water concentrations below 500 ppm to facilitate pipeline transport. The transport costs associated with capture may also vary. However, these are likely to be location specific, and depend more on the geography of the site and location relative to carbon storage locations and pipelines than the method used to capture the CO_2. Further differences in the final conditions and requirements of CO_2 would have an influence of the applicability of these models.

3.7 Project Finance Model

Several assumptions are made in the financial model for this project. The capital investment of the project was averaged over 3 years. The lifetime of the project was 30 years. The cost of capital was assumed to be 8%, with a discount rate of 12%. The built-in solver function in excel was used to adjust the electricity price so that the net present value of the project over the thirty-year lifetime was equal to zero.

3.8 Modeling Optimization

To find the optimal case, the "case study" feature in Aspen HYSYS was used to run simulations on variations on parameters. Case studies were run with different parameter in a nested fashion. This allowed to examine the impact different changing different system specifications had on the overall carbon capture system.

A short script in VBA was used to input the process data into a data calculation sheet for calculating the costs of process equipment and can be found in Appendix 17. The LCOE was calculated with Excel's solver function by setting the net present value to zero.

4 Results and Discussion

This chapter presents the results of the variables tested in the course of the simulation. Results are compared in plant performance, financial, and environmental metrics. A sensitivity analysis is conducted on some additional parameters to understand their influence on project costs.

4.1 The Influence of Sweep Flowrate

Typically, a sweep is used to decrease the membrane area. The introduction of a sweep decreases the partial pressures of components on the permeate side of the membrane, thereby promoting mass transfer across the membrane. While there is potential for some back-permeation across the membrane, choosing the right sweep gas that is not very permeable across the membrane can reduce the effect. As the membrane area goes down, the costs associated with membrane purchase, along with the lifetime replacements decreases.

Steam is chosen as the permeate gas for using the facilitate transport membranes. Having hydrated membranes helps promote the facilitated transport mechanism [37]. Steam is often readily available in process plants and can easily be separated from carbon dioxide later in the process.

However, to be in gaseous form at pressures above 1 bar, water needs to be heated above 100°C (212 °F). This increases a large amount of enthalpy into the system, which increases the cooling needs later in the process. Additionally, the introduction of a sweep gas increases the amount of compression needed slightly, as starting with the permeate of the first stage there is a larger quantity of gas present.

The results of varying sweep flowrate with a pure steam stream at 30°C are show in Figure 4-1. The conditions of this test are a target 1st stage recovery, $R_{CO2,1}$ of 92%, with an interstage pressure, $P_9=P_{10}$ of 6 bar without recompression (1st stage retentate and second stage feed are the same pressure).
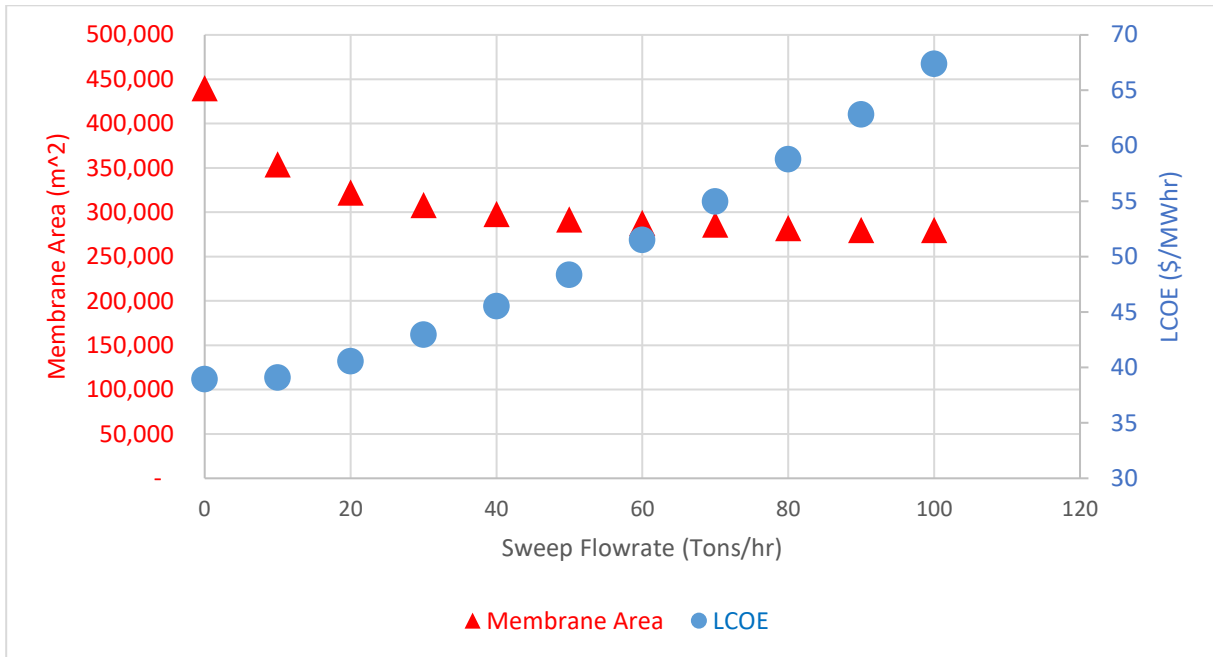
Figure 4-1: Results of changing sweep flowrate, F_5 on configuration A membrane area and LCOE.

As indicated in Figure 4-1, as flowrate increases, the membrane area decreases. The decrease in area is a first quick at lower sweep flowrates, but as the flowrate starts to exceed 80 tons/hr the decrease in impact can be noted as the membrane area starts to approach a minimum. The decrease in membrane area from the sweep is outweighed by the cost of other portions of the system increasing. Figure 4-2 offers insight to the reason behind the increase in cost. While the compression energy decreases with increasingly flowrate, the costs are outweighed by the significantly increased cooling need.
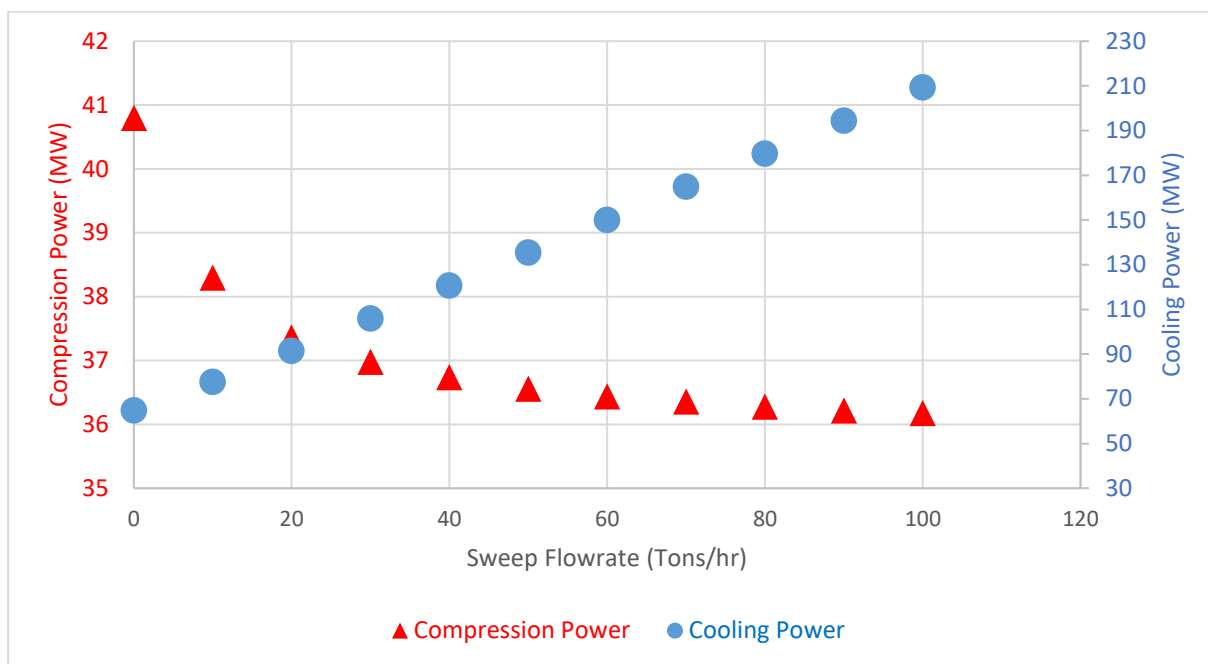
Figure 4-2: Results of changing of sweep flowrate, F_5 on configuration A compression and cooling power.

The increased cooling power requires increased capital and operational costs that increase the LCOE. Configuration B exhibited similar trends with an increase in cooling power and costs at higher flow rates. The graph of the results of configuration B can be found in Appendix 6.

4.2 Pressure Changes

In membrane processes, mass transfer can be either pressure limited, or selectivity limited, or a blend of the two. If mass transfer is pressure limited, increasing the pressure of the feed, or decreasing the pressure of the permeate, can promote further mass transfer due to the increase in driving force. If the mass transfer is selectivity limited, then increasing the pressure ratio does not provide a benefit.

Several locations in the system are suitable for pressure manipulation. The first examined is the recycle pressure. Increasing the recycle pressure increases the driving force across the membrane by increasing the partial pressure of CO_2 on the feed side of the membrane. In the layout of configuration, A, the feed pressure is expanded to meet the pressure of the recycle stream prior to introduction of the first membrane stage. Therefore, the effect of the decrease in compression requirements for the recycle compressor is overwhelmed by the increased compression need in other portions of the system.

In configuration A, the recycle goes back to the feed to the first membrane stage. Configuration B does not have a recycle stream, so the recompression instead goes to the boiler.

43
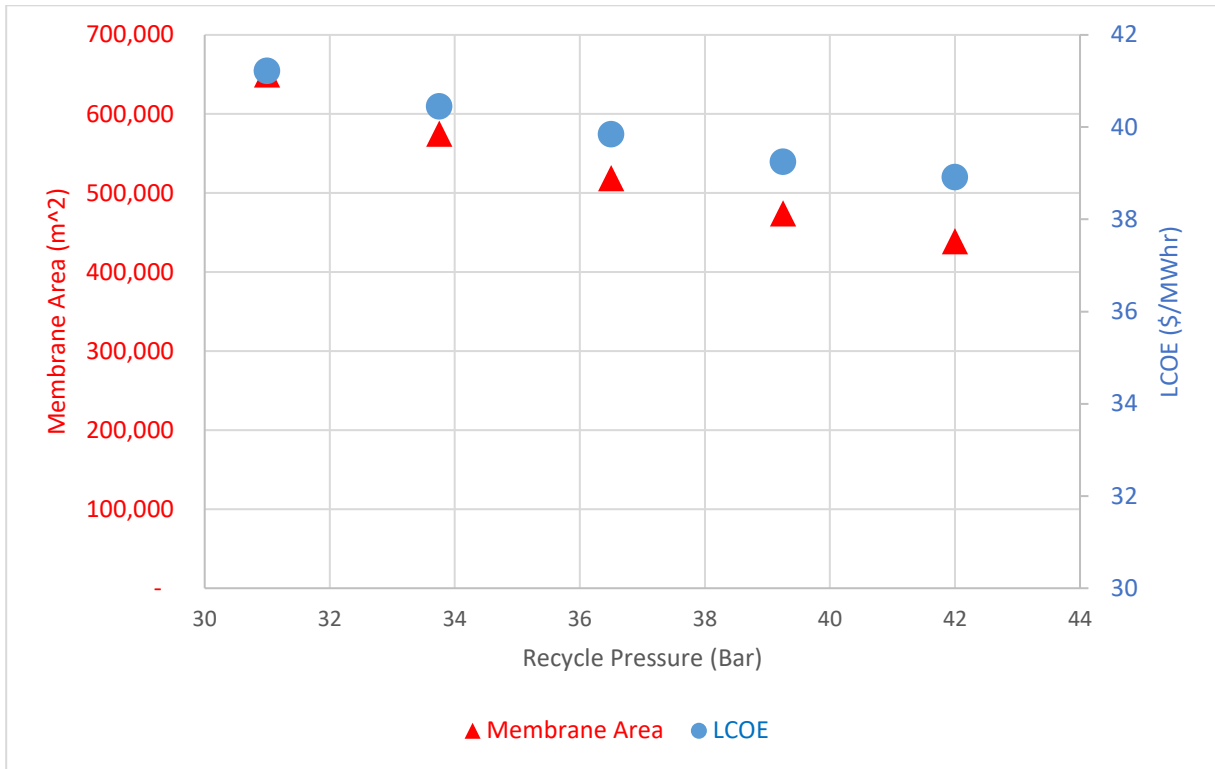
Figure 4-3: Results of changing configuration A recycle pressure, P_{16} on membrane area and LCOE.

The results for Figure 4-3 indicate as the membrane area and LCOE increasingly non-linearly as the recycle pressure increases.
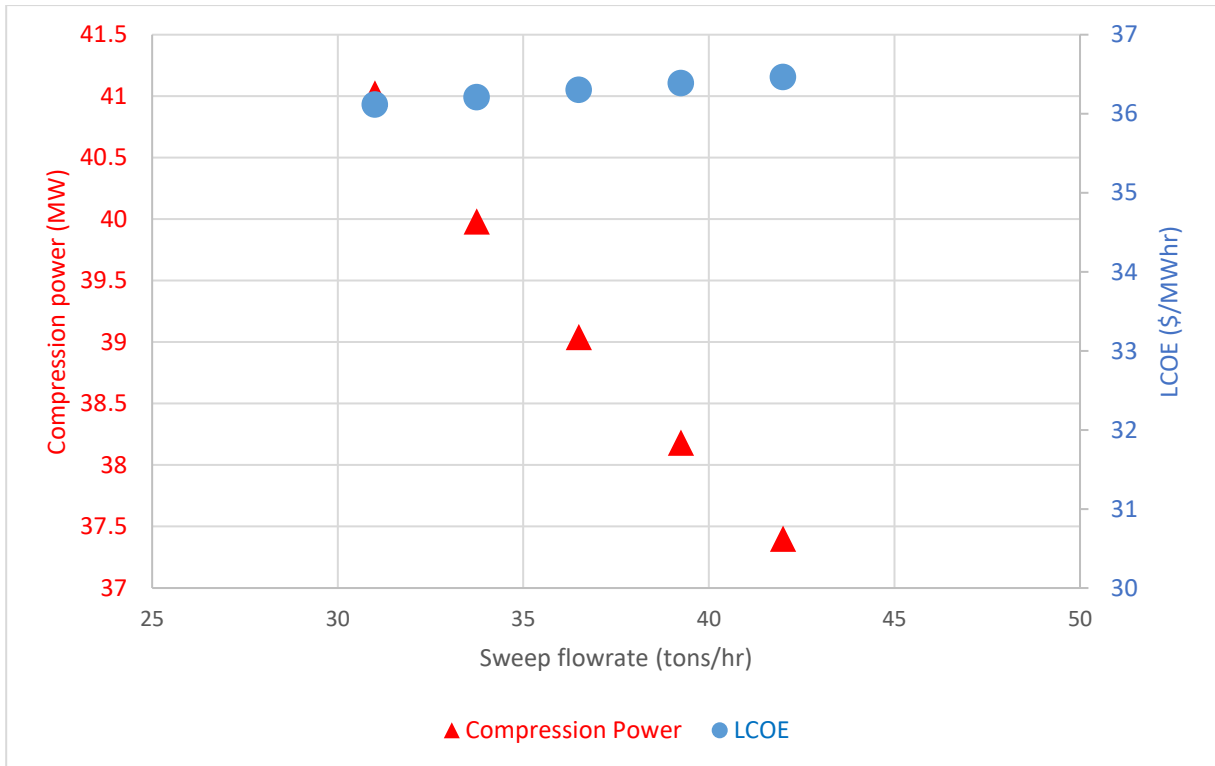
Figure 4-4: Results of changing configuration B recycle pressure, P_{16}, on compression power and LCOE

Configuration B, as reference in Figure 4-4, has a higher cost with higher recycle pressures. This is opposite the trend from configuration A, but this result can be explained as configuration B does not have a recycle, so any energy used in recompression is not beneficial for the system.

The next location analyzed is the effect of modifying the first stage retentate pressure (stream 9). The pressure of this stream is important because with a fixed feed pressure it determines the pressure ratio of the first stage. At high pressure permeate pressure, the pressure ratio is low, and the membrane is operating in the pressure ratio limited region, where changes in pressure influence the membrane area to a greater degree. As the permeate pressure decreases, the impact of the permeate pressure decreases as selectivity becomes the hindering item to mass transport. However, the membrane is only one portion of the system cost. While a low permeate pressure would be ideal for reducing the membrane area due to the high pressure ratio, it is less ideal for other portions of the system. Increased compression power begets increased cooling power due to the non-ideal work of the compression cycle. The impact of compressor size is especially important to the system. Not only do compressors require a large capital investment, which weighs more heavily in LCOE calculations due to occurring earlier in the plant lifetime, but they also use significant electricity, the most expensive utility.
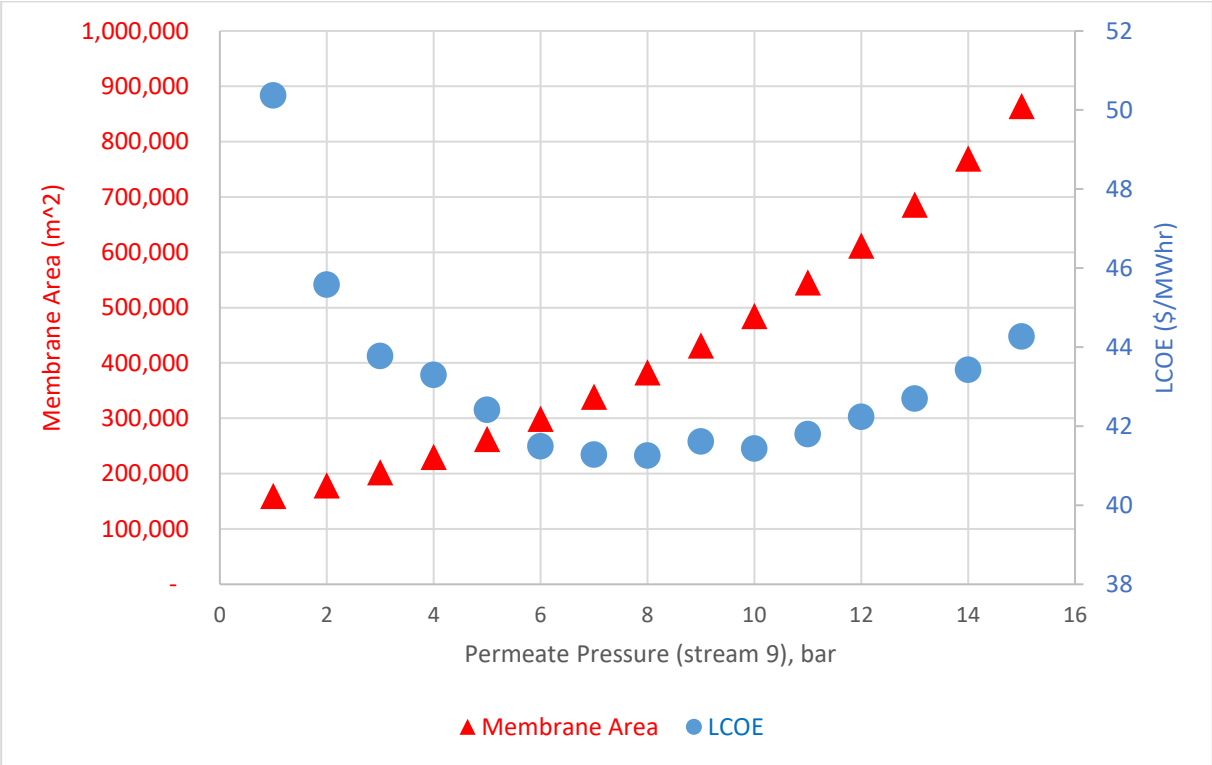
Figure 4-5: Results of changing configuration A first stage permeate pressure, P_9, on membrane area and LCOE.

Figure 4-5 indicates that a local minimum exists for the permeate pressure, P_9 within the range of between 6 and 10 bar when $R_{CO2,1}$ is fixed at .92, P_{10} at 16 bar, and P_{16} at 41 bar. Another observation from this Figure 4-5 is that there are some irregularities in the trend of the data when the P_9 = 9 bar. This can be explained by the

module-based costing approach use to size the compressors. As the maximum size of the compressor drives is 2600 kW, any compressors larger than this is modeled as multiple smaller compressor units, which have an overall higher total cost. As is emphasized in Table 4-1, at p_9 = 9 bar, the sizes of both K-102 and K-103 are just over the maximum power for a single compressor, so this unit has more compressor units than the adjacent pressures tested.

Table 4-1: Key compressor values when the retentate pressure, P_9, is near 9 bar and a maximum single compressor size of 2600 kW.

Pressure (Bar)	Total Compression Power (MW)	K-102 Power (kW)	K-103 Power (kW)	Number of Compressors
6	23.30	5,174	1,864	3
7	22.80	4,408	2,136	3
8	22.40	3,734	2,424	3
9	**22.08**	**3,123**	**2,728**	**4**
10	21.81	2,555	3,044	3
11	21.60	2,021	3,392	3

Another important location where pressure occurs is the recompression between the membrane stages. Much as the permeate pressure of the first membrane stage, P_9, determines the pressure ratio in the first stage, the recompression pressure, P_{10}, determines the pressure ratio in the second membrane stage as the permeate pressure, P_{18} is fixed to 1.1 bar. Likewise, the same tradeoff exists between developing sufficient driving force and the costs of compression.
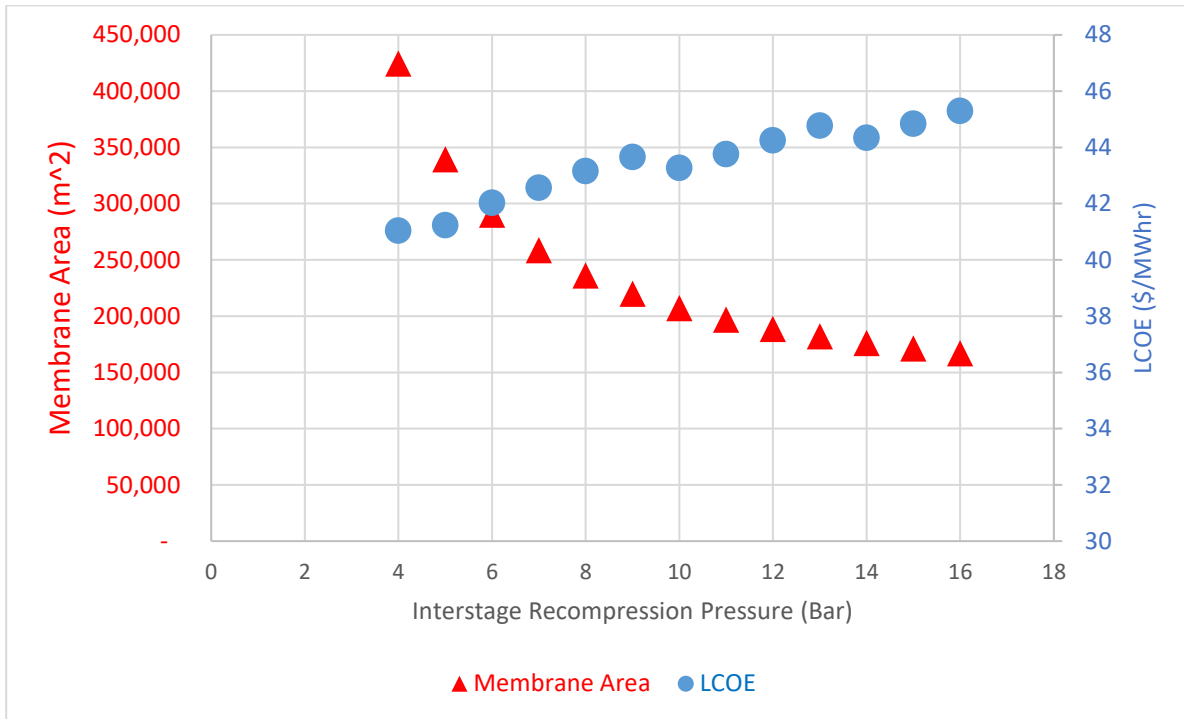
Figure 4-6: Results of changing interstage recompression pressure on cost and membrane area when the permeate pressure of the first stage, P_9 is equal to 2 bar.

Changing the interstage compression pressure with the initial permeate pressure equal to 2 bar indicated a decrease in membrane cost at lower recompression pressures. However, this is run at P_9 of 2 bar, which does appear to have a higher cost as indicated Figure 4-5 compared to slightly higher first stage permeate pressures. The trend for cost also exhibits the non-linear increases references in Figure 4-5. Similarly, this is due to an increase in the number of compression units required based on maximum size limits compare to the adjacent data points.

While Figure 4-6 on its own would appear to indicate that a lower recompression pressure leads to lower levelized cost, this does not take into account that operating at P_9 of 2 bar is suboptimal as indicated earlier in Figure 4-5. Therefore, it is important to evaluate other operating pressures.

A compression stage can be effectively eliminated by setting P_9 equal to P_{10}. In addition to eliminating the capital cost and energy usage, this has important implications on the system. The trade of in this situation is that the two membrane systems operate at different stage cuts depending on the interstage pressure. At low interstage pressures, a relatively high driving force in the first stage results in a smaller membrane area, and lower stage cut in the first stage. At higher interstage pressures, the lower driving force in the first stage requires a greater stage cut to achieve the desired 90% recovery. The greater stage cut also means that the membrane area increases. The trends for the second membrane stage are in reverse – the higher interstage pressure results in a higher driving force across the second stage, as the second stage permeate pressure, P_{18} is fixed at 1.1 bar.
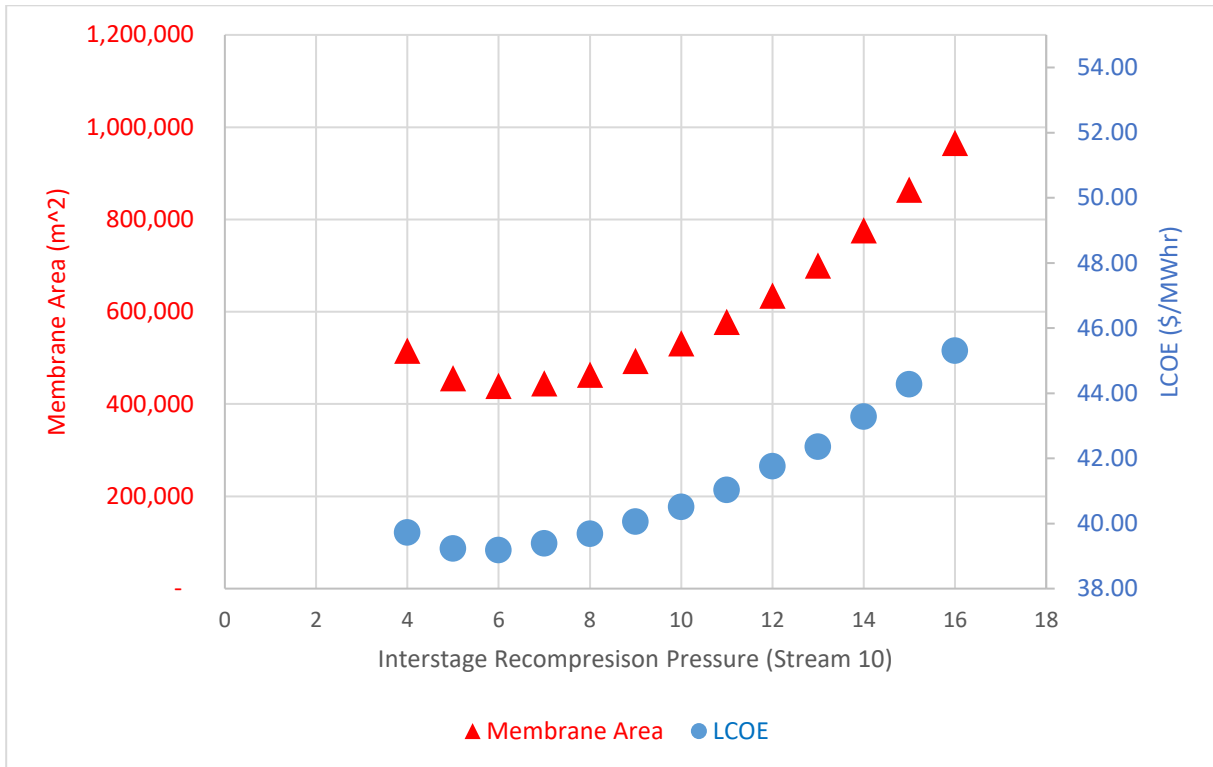
Figure 4-7: Results of changing interstage recompression when the first stage permeate pressure, P_9, is equal to the recompression pressure P_{10}

Figure 4-7 takes the image of cost at a first stage permeate pressure, P_9, is equal to the recompression pressure, P_{10}. The elimination of interstage recompression eliminates the need for K-102 and its associated heat exchanger. The data indicates that the membrane area and cost of electricity have a minimum near P_{10} = 6 bar. This is particularly interesting because it offers a simpler design and overall fewer unit compression units, while also providing a lower cost of the system. A similar trend can be expected in configuration B, which is also a two-membrane system. The results of the simulation for configuration B can be seen in Figure 4-8.
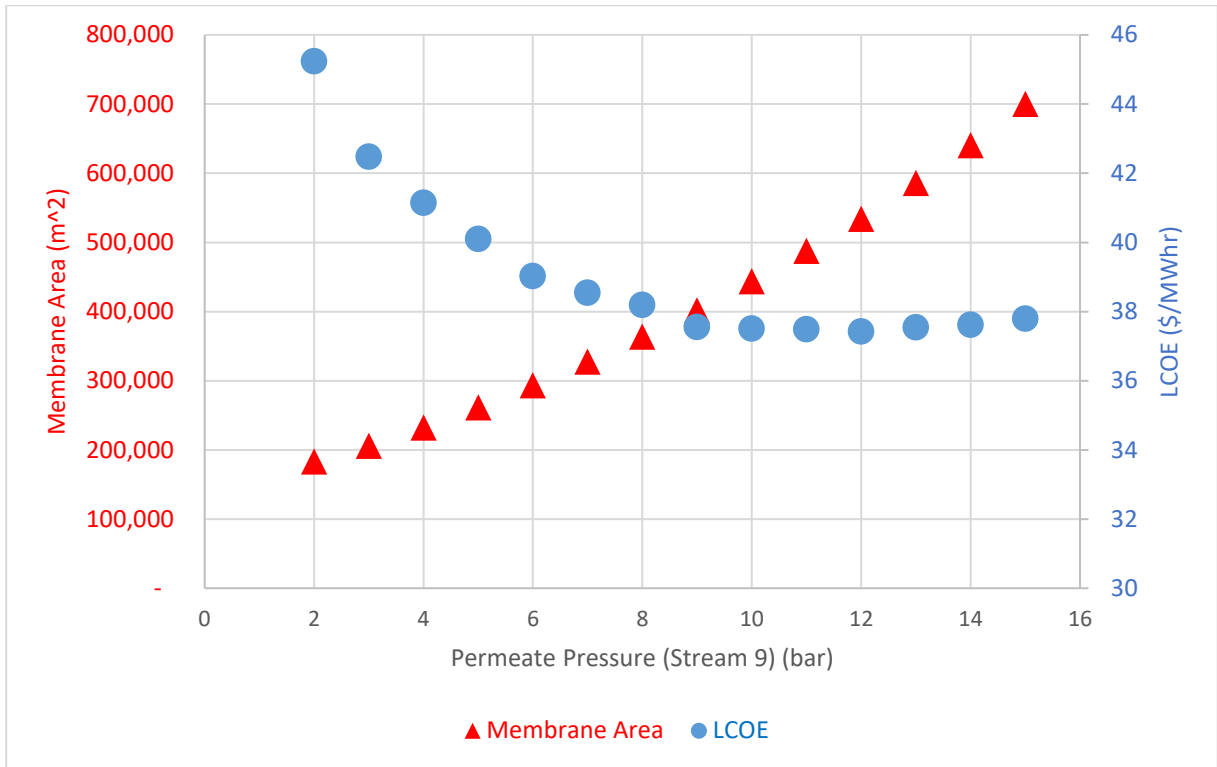
Figure 4-8: Results of changing interstage recompression when the first stage permeate pressure, P_9, is equal to the recompression pressure, P_{10}, in configuration B

The minimum is shifter, starting at P=8 bar, and is shifted to a higher pressure range. Since there is no recycle in this system, the separation needs to be converted in a single pass, and thus the system appears to favor a higher driving force across the second membrane stage.

4.3 CO_2 recovery and cost

The recovery of CO_2 is an important parameter in the simulation, as it determines both the amount of greenhouse gas that is released to the atmosphere, along with the energy required to achieve the separation. Having a lower CO_2 recovery is typically less costly, however, there are sometimes tax incentives or other contractual terms that require reaching a certain recovery of CO_2.
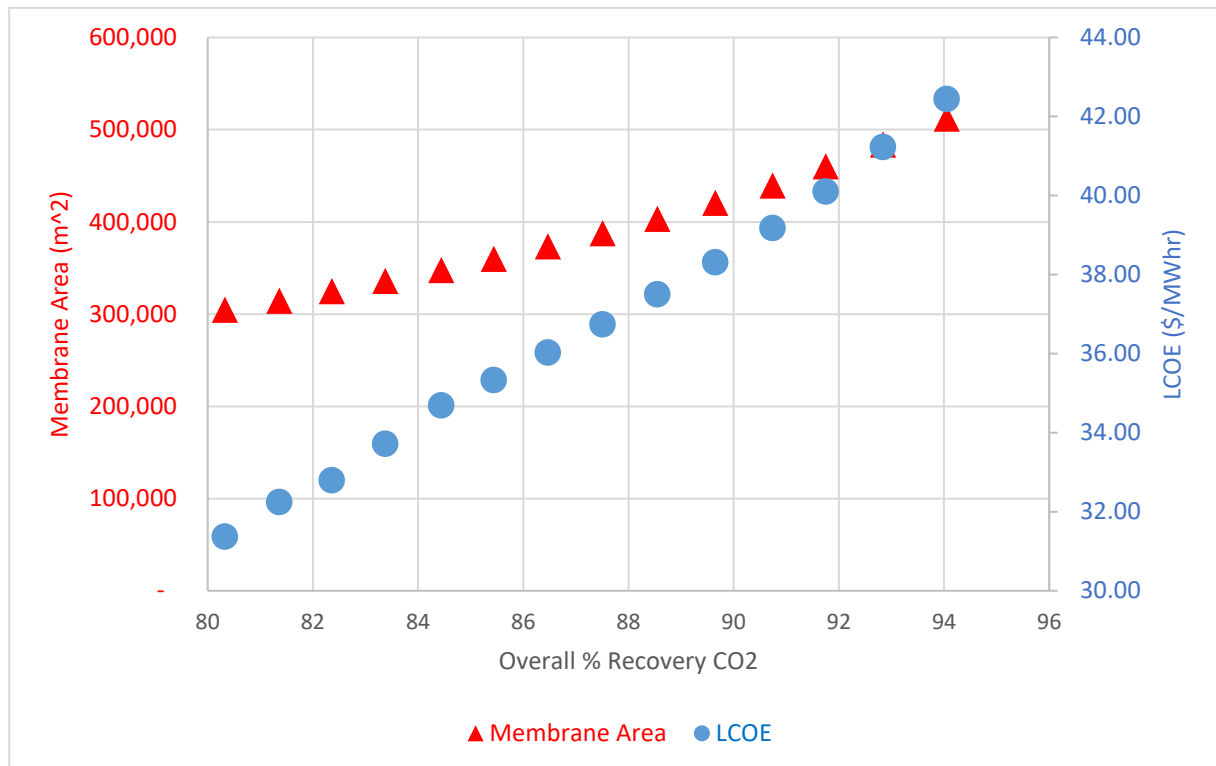
Figure 4-9: Results of changing ADJ-1 target on membrane area and LCOE.

Figure 4-9 indicates the results of changing the adj-1 target recovery, $R_{CO2,1}$, for first stage CO_2 recovery on membrane area and LCOE. For this scenario, as the CO_2 recovery increases, the hydrogen purity decreases, as there is more CO_2 in the H_2-stream fed to the boiler. The membrane area increases non-linearly with increasing recovery. The LCOE increase is slightly more linear. This could be due to the variety of costing parameters that go into the estimation of the levelized cost of electricity. Some, such as membrane cost, and electricity increase linearly as the costing parameter increases. Others, such as compressor cost, have the increase in cost decrease as size gets larger (with the exception of cases that require multiple compressors). Lastly, at higher recoveries, the higher energy usage decreases the available power.

4.4 Optimized Cost Scenarios

4.4.1 Configuration A

Of the scenarios tested, the optimized cost were found at the conditions presented in Table 4-2. The costs associatd with this scenario are analyzed further in this section.

Table 4-2: Conditions of lowest cost configuration

Parameter	Description	Units	Value
F_5	Flow of sweep (H_2O), stage 1	Tons/hr	0
P_{16}	Recycle recompression pressure	Bar	42
$X_{CO2,15}$	Mole fraction CO_2, recycle	-	0.4088
P_9	Stage 1 permeate pressure	Bar	6
P_{10}	Interstage recompression pressure	Bar	6
$R_{CO2,1}$	Stage 1 CO_2 recovery	%	92

The reuslts of the best case scenario can be evaluated in several ways. First, they could be evaluated on purely a cost basis. However, this does not capture the full picture of the process. Another import factor is the quality of the final products. While these targets are set as part of this report, a full financial analysis of the benefit at producing at different purity levels is not a part of the scope of this analysis.

Table 4-3: Quality results of configuration A best case compared to targets and baseline technology

Parameter	Target	Value	Selexol Baseline
H_2 recovery	>=95%	99.1%	99.8%
CO_2 recovery	>=90%*	90.7%	90.0%*
H_2 purity	>=85%	88.7%	91.2%
CO_2 purity	>=95%	98.1%	99.0%
$X_{H2O, CO2\ product}$	<500 ppm	250 ppm	500 ppm

As indicated in Table 4-3, the best case in configuration A meets the perofrmance requirements set out as targets for this report. However, in most cases the values acheived vary from the selexol baseline results.

The results can be further examined in terms of capital and operating costs. The capital costs for equipment type are collected in Table 4-4.

Table 4-4: Breakdown of capital equipment costs for case A optimized case

Equipment Type	Total Cost	Number of process units
Compressors/drives	$135,013,460	28
Heat Exchangers	$23,816,624	32
Membranes	$32,955,000	4
Vessels	$33,700,000	4
Total	$225,485,084	68

The compressors are the largest portion of the capital cost in this equation, followed by similar amounts for membrane equipment and process vessels. The large number of heat exchangers and compressors compared to other units is a result of the size limitations on equipment as described in Chapter 3. The breakdown of the compressors can be found in Appendix 7.

Table 4-5: Breakdown of capital equipment costs for case A optimized Case

Cost Type	Base Cost	Multiplier	Operational Cost
FCIL	$225,485,084	0.18	$40,587,315
Labor	$436,800	2.76	$1,205,568
Utilities	$45,376,603	1.23	$55,813,222
Total	**$271,298,488**	**-**	**$97,606,105**

Table 4-5 describes the operational costs associated with case A. The utility cost is driven mainly by the compression energy, which is $34 million compared to $11 million for the cooling water usage and energy. Labor, at less than $2 million contributes a relatively small portion of the total annual operating expenditures. This is based on the assumption that 6 operators, or approximately one operator per shift for 24/7 operation. The electricity used as a portion of the utility also has the added disadvantage of reducing the available capacity of the plant to produce revenue-generating power.

The optimal case can be examined in terms of carbon capture metrics presented in chapter 3, as seen in Table 4-6.

Table 4-6: Quality results of configuration A best case compared to targets and baseline technology

Parameter	Value
Net power (MW)	523
CO_2 captured (tons/year)	3,012,058
CO_2 emitted (tons/year)	307,380
LCOE with CO_2 capture	$147.04
Cost of CO_2 captured ($/ton)	$37.1
Cost of CO_2 avoided ($/ton)	$43.9
% LCOE Increase	36%
Breakeven CO_2 sales price ($/ton)	$101.05
Breakeven CO_2 penalty ($/ton)	$132.06

A key note is that the breakeven prices are based on a power generated cost of $64 per MWhr, which represents the base case of a traditional pulverized coal power plant. This results in the breakeven penalty and sales prices being higher than if they were based off of the power generation cost of another IGCC power configuration alone. Additionally, the breakeven sales price and penalty take into account the discount factor of 12%, which results in future revenues making less of an impact, further increasing the cost of the prices.

4.4.2 Configuration B

Of the scenarios tested within configuraiton B, the optimized cost were found at the conditions presented in Table 4-2. The costs associatd with this scenario are analyzed further in this section.

Table 4-7: Conditions of lowest cost scenario in configuration B

Parameter	Description	Units	Value
F_5	Flow of sweep (H_2O), stage 1	Tons/hr	0
P_{16}	Recycle recompression pressure	Bar	31
$X_{CO2,15}$	Mole fraction CO_2, recycle	-	.07
P_9	Stage 1 permeate pressure	Bar	8
P_{10}	Interstage recompression pressure	Bar	8
$R_{CO2,1}$	Stage 1 CO_2 recovery	%	92

The parameters in Table 4-7 can be compared to configuration A. Notably, the sweep flowrate is also the same at zero, and the compression pressure is equal to the permate pressure, indicating it is advantegous to complete the separation without interstage recompression. However, this scenario differs in having a benefiit from reducing the recycle recompression pressure, P_{16} as there is no need to generate a driving force from a recycle. The only requirement on this stream is to deliver fuel to the turbine at 31 bar.

Table 4-8: Quality results of configuration A best case compared to targets and baseline technology

Parameter	Target	Value	Selexol Baseline
H_2 recovery	>=95%	98.0%	99.8%
CO_2 recovery	>=90%*	90.1%	90.0%*
H_2 purity	>=85%	88.1%	91.2%
CO_2 purity	>=95%	96.3%	99.0%
$X_{H2O, CO2\ product}$	<500 ppm	250	500 ppm

As indicated in Table 4-8, the best case in configuration B also meets performance requirements. However, in this case the results are a bit lower than those in configuration A and the selexol process.

The results can be further examined in terms of capital and operating costs.

Table 4-9: Breakdown of capital equipment costs for case B optimal case

Equipment Type	Total Cost	Number of process units
Compressors/drives	$124,347,254	26
Heat Exchangers	$21,445,416	30
Membranes	$36,585,000	4
Vessels	$33,700,000	4
Total	$216,077,670	64

Compared to configuraiton A, configuration B has 2 fewer compressors and 2 fewer heat exchangers. The detailed size breakdwon of compressor

Table 4-10: Breakdown of capital equipment costs for case B optimal Case

Cost Type	Base Cost	Multiplier	Operational Cost
FCIL	$216,077,670	0.18	$38,893,981
Labor	$436,800	2.76	$1,205,568
Utilities	$41,176,791	1.23	$50,647,452
Total	**$257,691,260**		$90,747,001

Table 4-10 shows operational costs from configuration B. Similar to case B, electricity at $31 million accounts for the majority of the operational costs from utilities. The annual operating costs are $7 million less in case B due to lower compression and cooling energy requirements, and slightly less capital.

The optimal case can be examined in terms of carbon capture metrics presented in chapter 3, as displayed in Table 4-11. A notable trend both in this and the earlier results is that the cost of CO_2 captured, and the breakeven CO_2 sales price, are fairly different in cost, despite being similar metrics. This underscores the importance that different reporting methods have on the financial appearance of carbon capture technologies.

Table 4-11: Key carbon accounting metrics for configuration B optimal case

Parameter	Value
Net power (MW)	535
CO_2 captured (tons/year)	2,991,810
CO_2 emitted (tons/year)	327,629
LCOE with CO_2 capture	$143.99
Cost of CO_2 captured ($/ton)	$35.2
Cost of CO_2 avoided ($/ton)	$40.7
% LCOE Increase	33%
Breakeven CO_2 sales price ($/ton)	$100.28
Breakeven CO_2 penalty ($/ton)	$128.19

A discounted cash flow can be seen below in Figure 4-10. The initial capital investment casuses the cashflow to be negative. Starting in year 3, the plant is in revenue service, providing a source of income. After 33 years of operation, the net present value of the plant is zero in accordance with the LCOE calculations described in chapter 3.
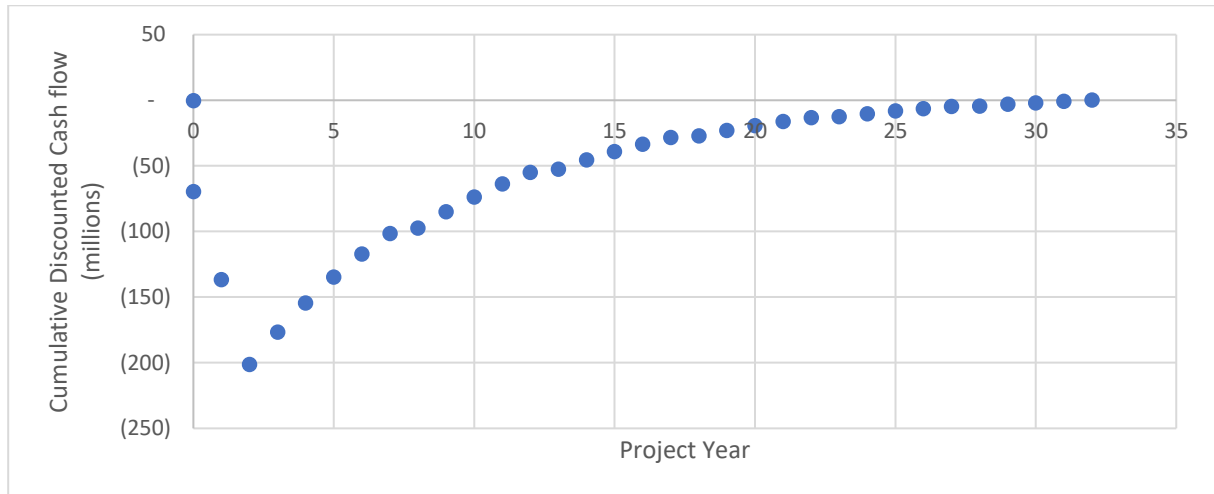
Figure 4-10: Cumulative discounted cash flow for configuration A minimum cost scenario

4.5   Comparison to Baseline Technology

To understand the relevance of this study, comparisons can be made to the Selexol process, as done in Table 4-12.

Table 4-12: Comparison of lowest cost scenarios to Selexol process

Item	B5B	Configuration A	Configuration B
Compression Power used	30	41	45
Other Power Used	24	65	63
Total Power	54	106	108
Capital Cost – Gas Separation Equipment (million)	$289	$80	$73
Capital Cost – CO_2 Compression and Cooling (million)	$72	$145	$143
Initial Solvent Fill (million)	$21	$0	$0
Total Construction Cost (million)	$382	$225	$216
% LCOE increase	31	36	33

A large difference is observed in the capital cost breakdown between the baseline case and the two ideal configurations presented in this analysis. The discrepancy can be traced for several reasons. First, the CO_2 output is delivered at two different pressures. Approximately 73% of the mass flow of the CO_2 stream is delivered at 5.5 bar, while the remaining CO_2 stream is delivered out of the Selexol unit at 1.2 bar [27]. In the proposed membrane processes, the entirety of the CO_2 stream is delivered at 1.2 bar. The large

percentage of the lower-pressure CO_2 compared Selexol process significantly increases the CO_2 compression needs, increasing the capital cost for compression equipment. As the increased compression also increases the cooling needs of the system, capital costs for heat exchangers increase as well. Different cost models also contribute to cost differences. The specific cost of compression equipment is approximately $3.3 million per MW in the cases presented compared to $2.4 million per MW in the Selexol base case [27]. Between the two cases analyzed, the lack of a recycle stream reduces the gas processing equipment costs in configuration B.

Further differences can be noted in the capital cost for separation equipment. The separation equipment of a membrane system is fairly simple, consisting of the membrane module plus any feed-side compression, handling, and cooling. In this case, separation equipment is considered to be the two membrane modules, interstage compressor and heat exchanger, water removal vessel, and recycle pump. In the Selexol process, the capital equipment is much more extensive, as it requires adsorption and regeneration columns, multiple flashing vessels, pumps, and heat exchangers as part of the process. Additionally, the initial solvent fill is estimated to cost $20 million alone, while the membrane system does not require any solvent.

4.6   Sensitivity Analysis

4.6.1 Membrane Cost

A sensitivity analysis is performed on the membrane cost to understanding the affect that this parameter has on the LCOE and carbon capture costs. As industrial scale facilitated transport membranes are not yet readily produced, it is important to understand that there is arrange of possibilities for the final cost of the membrane. Therefore, having a sensitivity analysis indicates how changes in price of the membrane may affect the overall process.

Another benefit of the sensitivity analysis is that it can serve as a proxy for increased membrane permeance. As the membrane permeance increases, the amount of membrane area needed for the same separation decreases. Therefore, the effective cost to achieve the separation decreases, in a similar way as if the membrane cost per unit area had decreased.

CO2 Penalty = $0.0961*C_M + 120.99$

LCOE Increase = $0.065*C_M + 31.214$

- LCOE increase
- Breakeven CO2 sales price
- Breakeven CO2 penalty
- .... Linear (LCOE increase)
- .... Linear (Breakeven CO2 penalty)
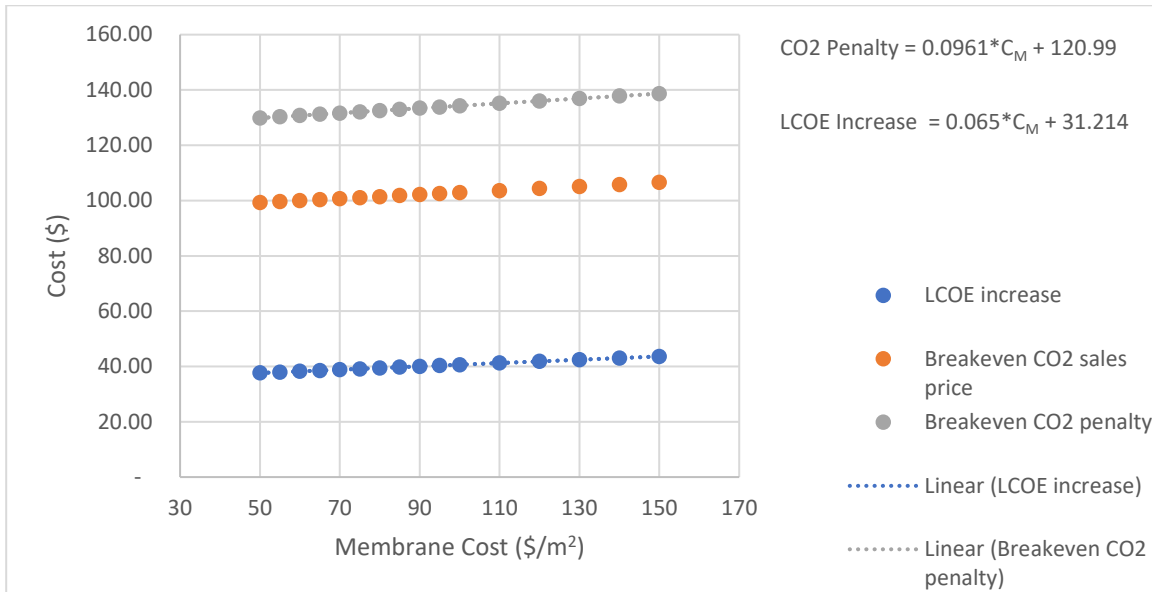
Figure 4-11: Sensitivity Analysis of Membrane Cost in Configuration A

Figure 4-11 shows the sensitivity of key cost metrics to the price of membrane. For every $1 change in C_{spef}, the LCOE is expected to change $.065, and the breakeven CO_2 penalty is expected to change $.096. This relationship is linear due to the linear nature of the membrane cost, and the small change per dollar of membrane due to the fact that the membrane capital expenditure is only a small portion of the total capital cost.

4.6.2 Discount Rate

An important economic factor in the simulation is the discount rate. At higher discount rates, future revenues and expenses have lesser impact. As inflation and interest rates have risen over the past year, it is important to understand how broader conditions within the economy can effect the finacnial viability of carbon capture projects. With a lower discount rate, future costs have greater value. At a higher discount rate, such as might be required in periods with high inflation where a greater return on invesment is sought, the future returns have lower importance. Since it is assumed that during the first three years of plant life construction is occuring with both considerable capital investment and no operating revenue, a higher discount rate requires later revenues to be greater to offset the costs. The sensititivity analyis in Figure 4-12 indicates this trend, as the LCOE can range from a price of $29 with no discount rate, to $48 with a discount rate of 20%.
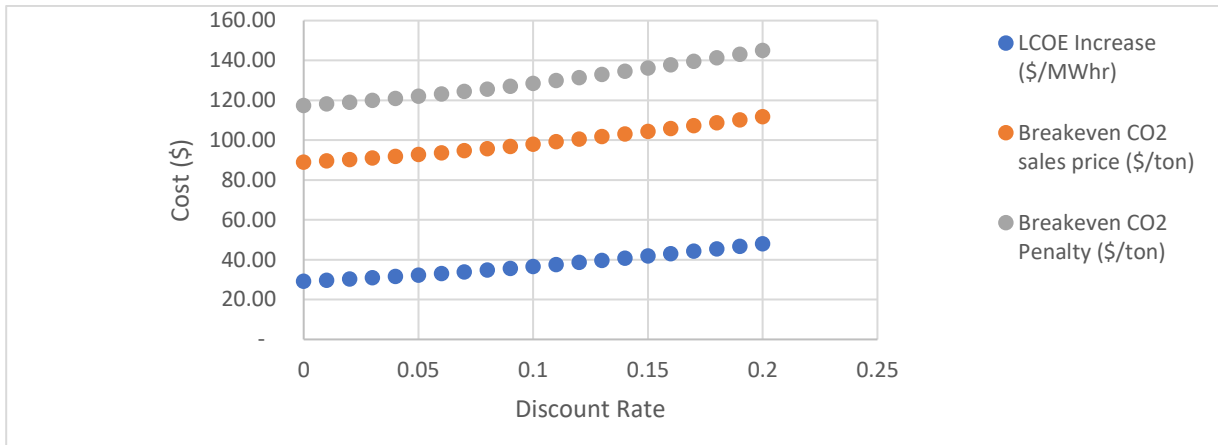
Figure 4-12: Sensitivity Analysis of Discount Rate in Configuration A

Figure 4-12 shows the sensitivity analysis of the discount rate. Both the LCOE increase, and the breakeven CO_2 penalty show an exponential relationship a change in discount rate. As the discount rate increases, the loss of value in future revenues increases exponentially, and therefore, an exponential increase in cost is also needed to offset the real value of returns.

4.6.3 Sales Price of CO_2

In the base case, it is assumed that selling CO_2 does not generate any revenue. However, viable uses do exist for capture CO_2, including in packaged foods, enhanced oil recovery [55]. If the capture CO_2 could be put to use in one of these secnarios, the economics of the process change. The sales price refers to the price received by the power generation facilitiy, or the revnue. All transport costs (estimated at $10/ton) are assumed to be paid by the buyer on top of the sale price.

Often, the cost of CO_2 is pegged to the price of oil[56]. This economic incentive promotes more effective outcomes, as CO_2 production is incentivized when the price of oil is high, and when oil prices fall encourage to cut back [57]. However, this makes financial modeling more difficult. A fixed price of CO_2 can be used to provide a simple analysis of the impact that CO_2 sale price has on process economics and understand the picture of the relative importance of the change in price to the price of electricity. As the sales price of CO_2 goes up, the LCOE would be expected to drop. The price of CO_2 is ranged from $0 to 30 per ton, with the resulted depicted in Figure 4-13.

Figure 4-13: Effect of sale price of CO_2 on LCOE

Two noteworthy trends can be observed in this figure. First, at higher sale prices of CO_2, the slope of the cost vs. the % recovery is lower. This indicates that as the sales price of CO_2 goes up, the price premium on achieve higher recoveries is reduced. The second is that while the breakeven sale price of CO_2 for the configuration A minimum was $101/MWhr as indicated in Table 4-8, the LCOE increase drops to less than $15/MWhr with a CO_2 sales price of $30/ton. This underscores the important role that the carbon capture metrics play – While the LCOE increase is using a base price of $107/MWhr for an IGCC power plant with no carbon capture, the breakeven CO_2 sales price assumes the price for a pulverized coal plant of $64 per MWhr. Therefore, it is important to appreciate the impact metrics play in shaping how cost data can be interpreted with carbon capture.

5 Conclusion

5.1 Summary

This report examined carbon-capture using membrane technology in an integrated gasification combined cycle power plant application. Two process configurations were analyzed; one with a recycle and the other without. Quality assumptions were outlined with the required CO_2 and H_2 recoveries, purities, and contaminant levels.

The best-case scenario with the recycle provided electricity at a levelized cost of/MWhr, a 36 % increase over a baseline case, while the alternative without recycle provided electricity at 143.99/MWhr, or a 33% increase. However, the slight improvement in hydrogen recovery and CO_2 purity provided by the recycle, and the minimal increase in cost mean that this configuration could be preferred if increased purity is needed.

Several parameters were explored for their influence on the process economics. It was found that minimizing the sweep flowrate of steam was beneficial to reducing cost. Similarly, it was advantageous to set the first stage permeate pressure equal to the interstage recompression pressure, thereby eliminating a compressor and heat exchanger unit. Lastly, the recompression pressure for the recycle was explored, and found that increasing the recycle pressure up to the feed pressure was beneficial for reducing cost. A sensitivity analysis was performed on the key parameters of membrane cost, discount rate, and CO_2 sale price to understand their potential impact on the process.

The results of the financial analysis compare similarly with baseline adsorption technology. The 33% increase in levelized cost of electricity for carbon capture with the facilitated transport membrane system is close to reaching the 31% increase in cost for the baseline adsorption technology.

6 Potential Further Work

Improved optimization of the CO_2 compression and interstage membrane compression could be examined for improved performance. As carbon capture continues to mature, improvements in technology related to CO_2 compression can be applied to membrane systems. As compression equipment is the largest part of the capital cost, reduction in compression energy needed would also minimize the levelized cost of electricity. Improvements to facilitated transport membranes could serve as another pathway to reducing compression needs and are worth more exploration. In particular, investigation into extending the benefit of facilitated transport into higher pressure operation could prove useful in an IGCC application that could operate at a pressure up to 42 bar.

More robust financial models could be created, with a deeper understanding of the different financial parameters involved in project cost estimation and a thorough analysis of how these factors influence the profitability of a project. Additionally, research into available tax credits and their applicability to carbon capture projects could provide more insight into scenarios where carbon capture is economically justifiable. As energy prices have risen over the past year, incorporating updated prices on coal and expected prices for energy could provide more insight into if an IGCC power plant would be economically viable.

Improved water management techniques could also be explored, with alternate technologies to the flashing of water to remove excess water from the process examined. Water management is also important to the membrane, and more detailed investigation of the effect of relative humidity on facilitated transport membranes at the elevated pressures found within IGCC applications could be explored.

Improvements in both membrane permeability, cost, and selectivity would all be future developments that should be investigated to see the impact on the overall cost of electricity. These parameters could be developed into detailed financial models to understand how future technology advances will affect implementation costs. While the discounted cash flow and net present value analysis assumes steady prices of key costs and revenues, in reality these prices are ever changing. Further research could be invested in developing more detailed financial models on how changes in major input parameters, such as coal prices, and revenue parameters, such as electricity and CO_2 prices, affect the finances of carbon capture projects.

Further research could also go into the effect of utilizing a membrane-based system on the overall system costs associated with the powerplant. For example, if H_2S can be co-sequestered with CO_2, there may be additional costs savings associated with the removal of H_2S processing equipment within the power plant. Other factors, such as land area required, and emissions should also be examined with membrane systems compared to other methods of carbon capture.

Further research could also go into areas to identify and address potential operational concerns with membrane systems. These include identifying the impact of the presence of hydrogen in metallic system components and getting additional information on operational profile over a membrane over the course of its lifetime.

As this case modeled just one size of power plant based on available data, other plant sizes could be examined to see if they are more economical with membrane systems. Alternative gasification and combustion technologies could also be examined. Facilitated transport membranes could be examined in other gas separation applications that have similar concentrations of CO_2 within the gas stream.

With any industrial application, safety and the environment are critical considerations. Further research could be conducted into identify potential risks associated with the operation and maintenance of carbon capture systems for IGCC power plants. Both the syngas (flammability) and presence of carbon monoxide (asphyxiation) present inherent risks associated with the carbon capture process. Additionally, the elevated pressures and temperatures in this process present risks as well. Therefore, it is important that safety considerations are made in the design and development of membrane systems for carbon capture to ensure that it is a safe system. Effects on the environment, such as potential chemical releases or other effects of industrial accidents, should be considered in this analysis.

References

References

1.   McMichael, A.J., R.E. Woodruff, and S. Hales, *Climate change and human health: present and future risks.* The Lancet, 2006. **367**(9513): p. 859-869.
2.   Ogunbode, C.A., R. Doran, and G. Böhm, *Exposure to the IPCC special report on 1.5 °C global warming is linked to perceived threat and increased concern about climate change.* Climatic Change, 2020. **158**(3): p. 361-375.
3.   Newell, R., D. Raimi, and G. Aldana, *Global energy outlook 2019: the next generation of energy.* Resources for the Future, 2019: p. 8-19.
4.   Wilcox, J., *Carbon capture*. 2012: Springer Science & Business Media.
5.   Manne, A. and R. Richels, *On stabilizing CO2 concentrations – cost‐effective emission reduction strategies.* Environmental Modeling & Assessment, 1997. **2**(4): p. 251-265.
6.   Breault, R.W., *Gasification processes old and new: a basic review of the major technologies.* Energies, 2010. **3**(2): p. 216-240.
7.   Cebrucean, D., V. Cebrucean, and I. Ionel, *CO2 Capture and Storage from Fossil Fuel Power Plants.* Energy procedia, 2014. **63**: p. 18-26.
8.   Lindsey, R. *Climate Change: Atmospheric Carbon Dioxide*. 2021 [cited 2021 12/14/2021]; Available from: https://www.climate.gov/news-features/understanding-climate/climate-change-atmospheric-carbon-dioxide.
9.   Deng, L. and H. Kvamsdal, *CO2 capture: Challenges and opportunities.* Green Energy & Environment, 2016. **1**(3): p. 179.
10.   Mulder, M., *Basic principles of membrane technology.* 1996.
11.   Strathmann, H., L. Giorno, and E. Drioli, *An Introduction to Membrane Science and Technology.* Consiglio Nazionale delle Ricerche, 2011.
12.   Dortmundt, D. and K. Doshi, *Recent developments in CO2 removal membrane technology.* UOP LLC, 1999. **1**.
13.   He, X., *A review of material development in the field of carbon capture and the application of membrane-based processes in power plants and energy-intensive industries.* Energy, Sustainability and Society, 2018. **8**(1): p. 34.
14.   Ma, Y., et al., *Hydrogen sulfide removal from natural gas using membrane technology: a review.* Journal of materials chemistry. A, Materials for energy and sustainability, 2021. **9**(36): p. 2211-224.
15.   Baker, R., *Membrane Technology and Applications*. 3. Aufl. ed. 2012, New York: New York: Wiley.
16.   Roussanaly, S. and R. Anantharaman, *Cost-optimal CO2 capture ratio for membrane-based capture from different CO2 sources.* Chemical Engineering Journal, 2017. **327**: p. 618-628.
17.   Grainger, D. and M.-B. Hägg, *Techno-economic evaluation of a PVAm CO2-selective membrane in an IGCC power plant with CO2 capture.* Fuel (Guildford), 2008. **87**(1): p. 14-24.
18.   Nagumo, R., S. Kazama, and Y. Fujioka, *Techno-economic evaluation of the coal-based integrated gasification combined cycle with CO2 capture and storage technology.* Energy procedia, 2009. **1**(1): p. 4089-4093.
19.   Ku, A.Y., et al., *Membrane performance requirements for carbon dioxide capture using hydrogen-selective membranes in integrated gasification combined cycle (IGCC) power plants.* Journal of Membrane Science, 2011. **367**(1): p. 233-239.
20.   Merkel, T.C., M. Zhou, and R.W. Baker, *Carbon dioxide capture with membranes at an IGCC power plant.* Journal of membrane science, 2012. **389**: p. 441-450.

21.   Han, Y. and W.S.W. Ho, *Facilitated transport membranes for H2 purification from coal-derived syngas: A techno-economic analysis.* Journal of membrane science, 2021. **636**(C): p. 119549.
22.   Scholes, C.A., et al., *Membrane Gas Separation – Physical Solvent Absorption Combined Plant Simulations for Pre-combustion Capture.* Energy Procedia, 2013. **37**: p. 1039-1049.
23.   Janakiram, S., et al., *Two-stage membrane cascades for post-combustion CO2 capture using facilitated transport membranes: Importance on sequence of membrane types.* International Journal of Greenhouse Gas Control, 2022. **119**: p. 103698.
24.   Filippov, S. and A. Keiko, *Coal gasification: at the crossroad. Technological factors.* Thermal Engineering, 2021. **68**(3): p. 209-220.
25.   Voldsund, M., K. Jordal, and R. Anantharaman, *Hydrogen production with CO2 capture.* International Journal of Hydrogen Energy, 2016. **41**(9): p. 4969-4992.
26.   Abadie, L.M. and J.M. Chamorro, *The Economics of Gasification: A Market-Based Approach.* Energies, 2009. **2**(3).
27.   James III PhD, R.E., et al., *Cost and Performance Baseline for Fossil Energy Plants Volume 1: Bituminous Coal and Natural Gas to Electricity*. 2019: United States. p. Medium: ED.
28.   Kazemifar, F., *A review of technologies for carbon capture, sequestration, and utilization: Cost, capacity, and technology readiness.* Greenhouse gases: science and technology, 2021.
29.   Zhang, X., et al., *Carbon chain analysis on a coal IGCC—CCS system with flexible multi-products.* Fuel processing technology, 2013. **108**: p. 146-153.
30.   Cardew, P. and M. Le, *Membrane Processes: A Technology Guide*. Vol. 238. 1998: Royal Society of Chemistry.
31.   Dai, Z., L. Ansaloni, and L. Deng, *Recent advances in multi-layer composite polymeric membranes for CO2 separation: A review.* Green Energy & Environment, 2016. **1**(2): p. 102-128.
32.   Wijmans, J.G. and R.W. Baker, *The solution-diffusion model: a review.* Journal of Membrane Science, 1995. **107**(1): p. 1-21.
33.   Janakiram, S., et al., *Three-phase hybrid facilitated transport hollow fiber membranes for enhanced CO2 separation.* Applied Materials Today, 2020. **21**: p. 100801.
34.   Saeed, M., et al., *Tailoring of water swollen PVA membrane for hosting carriers in CO2 facilitated transport membranes.* Separation and purification technology, 2017. **179**: p. 550-560.
35.   Ho, W. and K.K. Sirkar, *Membrane handbook.* 1992.
36.   Janakiram, S., et al., *Field trial of hollow fiber modules of hybrid facilitated transport membranes for flue gas CO2 capture in cement industry.* Chemical Engineering Journal, 2021. **413**: p. 127405.
37.   Deng, L., T.-J. Kim, and M.-B. Hägg, *Facilitated transport of CO2 in novel PVAm/PVA blend membrane.* Journal of Membrane Science, 2009. **340**(1): p. 154-163.
38.   Kim, T.J., B. Li, and M.B. Hägg, *Novel fixed‐site–carrier polyvinylamine membrane for carbon dioxide capture.* Journal of Polymer Science Part B: Polymer Physics, 2004. **42**(23): p. 4326-4336.
39.   Belaissaoui, B., et al., *Analysis of CO2 Facilitation Transport Effect through a Hybrid Poly (Allyl Amine) Membrane: Pathways for Further Improvement.* Membranes, 2020. **10**(12): p. 367.
40.   Rafiq, S., L. Deng, and M.B. Hägg, *Role of facilitated transport membranes and composite membranes for efficient CO2 capture–a review.* ChemBioEng Reviews, 2016. **3**(2): p. 68-85.
41.   Freeman, B., Y. Yampolskii, and I. Pinnau, *Materials science of membranes for gas and vapor separation*. 2006: John Wiley & Sons.

42. Marius, S., et al., *An integrated materials approach to ultrapermeable and ultraselective CO2 polymer membranes.* Science (American Association for the Advancement of Science), 2022. **376**(6588): p. 90-94.
43. Robeson, L.M., *The upper bound revisited.* Journal of membrane science, 2008. **320**(1): p. 390-400.
44. Lin, H., et al., *Plasticization-Enhanced Hydrogen Purification Using Polymeric Membranes.* Science, 2006. **311**(5761): p. 639-642.
45. Deng, L. and M.-B. Hägg, *Techno-economic evaluation of biogas upgrading process using CO2 facilitated transport membrane.* International journal of greenhouse gas control, 2010. **4**(4): p. 638-646.
46. Turton, R., *Analysis, synthesis, and design of chemical processes*. 4th ed. Prentice Hall international series in the physical and chemical engineering sciences. 2013, Upper Saddle River, N.J: Pearson Education.
47. van der Spek, M., S. Roussanaly, and E.S. Rubin, *Best practices and recent advances in CCS cost engineering and economic analysis.* International Journal of Greenhouse Gas Control, 2019. **83**: p. 91-104.
48. Grainger, D., *Development of carbon membranes for hydrogen recovery.* 2007.
49. Xu, W., *Labratory Data: Membrane Performance*. 2022.
50. Sandru, M., et al., *Pilot Scale Testing of Polymeric Membranes for CO2 Capture from Coal Fired Power Plants.* Energy Procedia, 2013. **37**: p. 6473-6480.
51. Yuan, M., et al., *Design and operations optimization of membrane-based flexible carbon capture.* International Journal of Greenhouse Gas Control, 2019. **84**: p. 154-163.
52. Stolecka, K. and A. Rusin, *Analysis of hazards related to syngas production and transport.* Renewable Energy, 2020. **146**: p. 2535-2555.
53. Manahan, J.M., et al. *Installation and maintenance challenges of NEMA Type 7 hazardous area enclosures*. in *Industry Applications Society 60th Annual Petroleum and Chemical Industry Conference*. 2013.
54. *Economic Indicators*, in *Chemical Engineering*. 2021. p. 48.
55. Ferguson, R.C., et al., *Storing CO2 with enhanced oil recovery.* Energy Procedia, 2009. **1**(1): p. 1989-1996.
56. Agarwal, A., *Risk sharing in CO2 delivery contracts for the CCS-EOR Value chain.* MIT Center for Energy and Environmental Policy Research, Massachusetts, USA, 2014.
57. Gao, S. and K. van 't Veld, *Pegging input prices to output prices—A special price adjustment clause in long-term CO2 sales contracts.* Energy Economics, 2021. **104**: p. 105619.

Appendices

Appendix 1: Risk Assessment

RISK ASSESSMENT (RiskManager alternative)

Unit/Institute:	IKP					Date:	26/1/2022	
Responsible line manager (name):	Liyuan Deng, Arrne Lindbrathen					Revised:		
Responsible for activities being risk assessed (name):	Ben Reeber							
Participants in the risk assement (names):	Ben Reeber							

Description of the activity, process, area, etc.:
The risk assement applies to the writing of the master's thesis. The thesis does not involve any laboratory work.

Activity / process	Unwanted incident	Existing risk reducing measures	Probability (P)	Consequence (C) Evaluate the categories individualley. *Health should always be evaluated.*				Risk value (P x C)	Risk reducing measures - suggestions Measures reducing the probability of the unwanted incident happening should be prioritized.	Residual risk after measures being implemented
			(1-5)	Health (1-5)	Material values (1-5)	Environment (1-5)	Reputation (1-5)			
Plugging in and using electrical devices in office such as laptops, phones, batteries, lights	*Electrical shock for electrical equipment.*	*Proper use of outlets and eletrical equipment.*	*1*	*1*	*1*	*1*	*1*	*1*	*Check cords ocassionally to ensure they are in good coniditon.*	1 (P = 1)
Walking into the office	*Tripping*	*Keep aisleways clear of bags and equipment.*	2	2	1	1	1	4	*Keep equipment free of aisleways*	2 (P=1)
Working in office	*Accident, fire, or chemical release in building*	*Fire drills, laboratory procedures.*	1	4	4	4	4	4	*Be aware of emergency exits and alarms*	4 (P=1)
Working in office	*Burn from office heaters*		1	2	1	1	1	2	*Avoid touching heaters directly*	2 (P=1)
Working in office	*Additional stress from masters thesis*	*Mental health support for students.*	2	2	1	1	1	2	*Proper planning and timeline of work*	4 (P=2)
Working in office	*Illness or infection*	*Frequent washing of hands. Follow proper infection control procedures.*	3	3	1	1	1	9		9 (P=3)
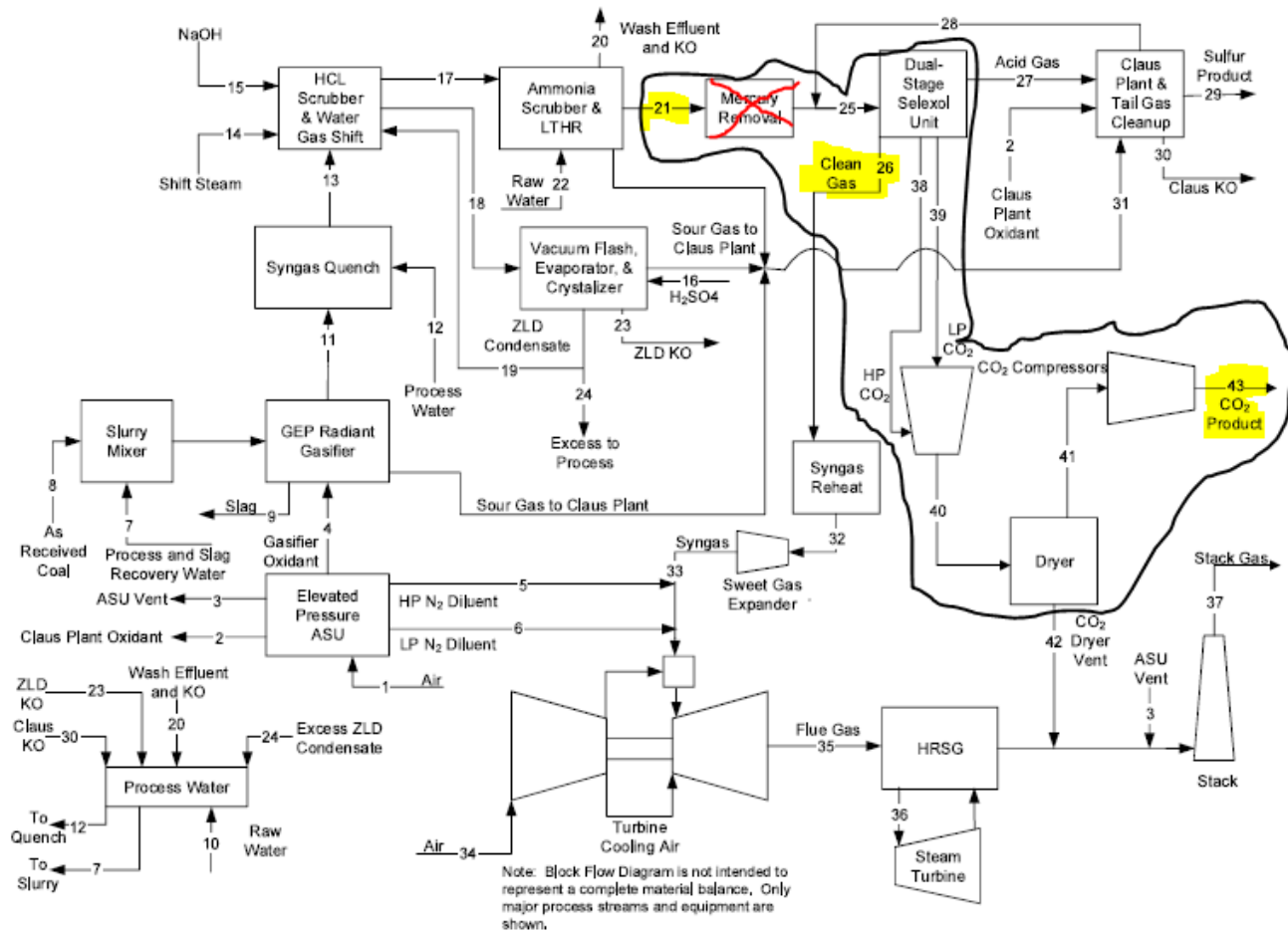
The system boundary, outlined in black, represents the portion of the power generation process that is examined in this scenario. Key streams are highlighted, 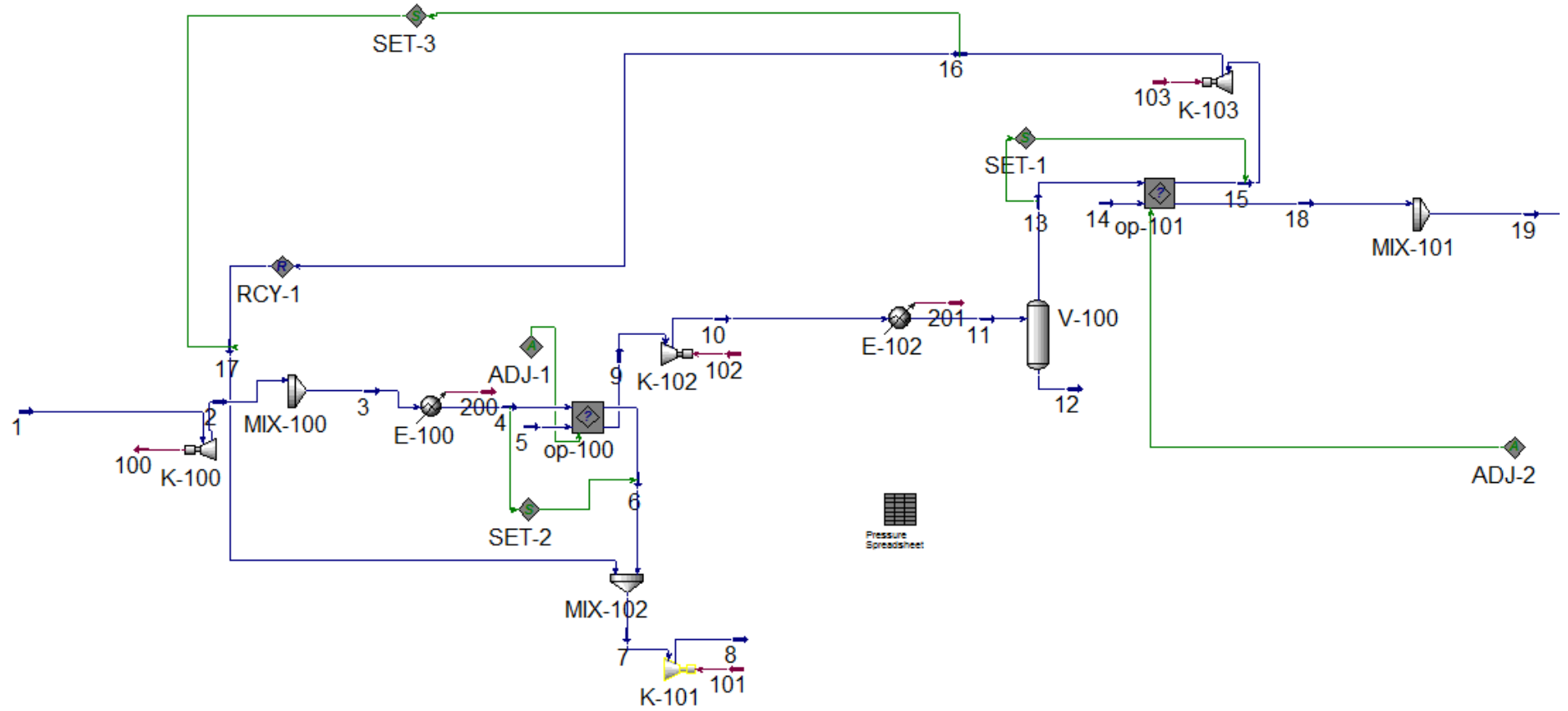included stream 21 (feed), stream 26 (syngas product) and stream 43 (CO₂ product). Excluded are analysis of the mercury removal of the process, which can be assumed to be relocated elsewhere.
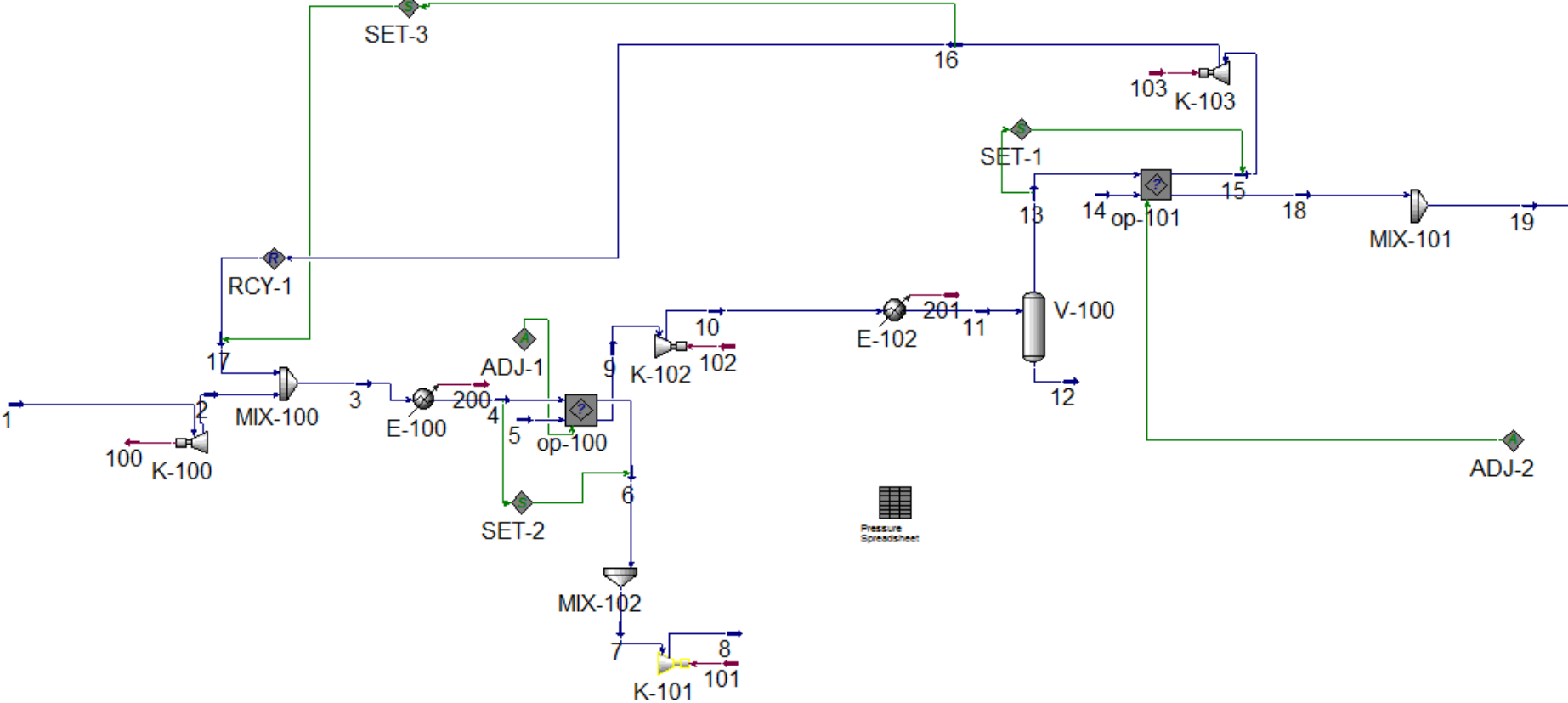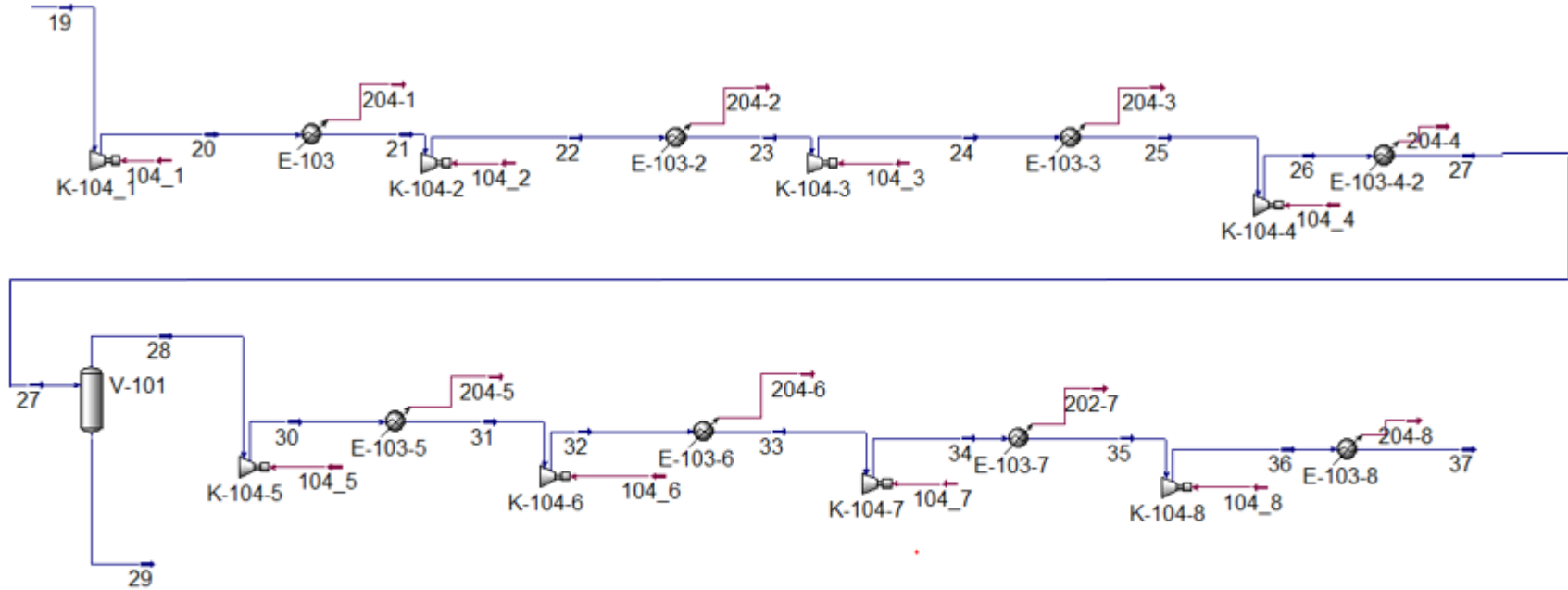
Appendix 6: Results from configuration B with varying sweep gas flowrate
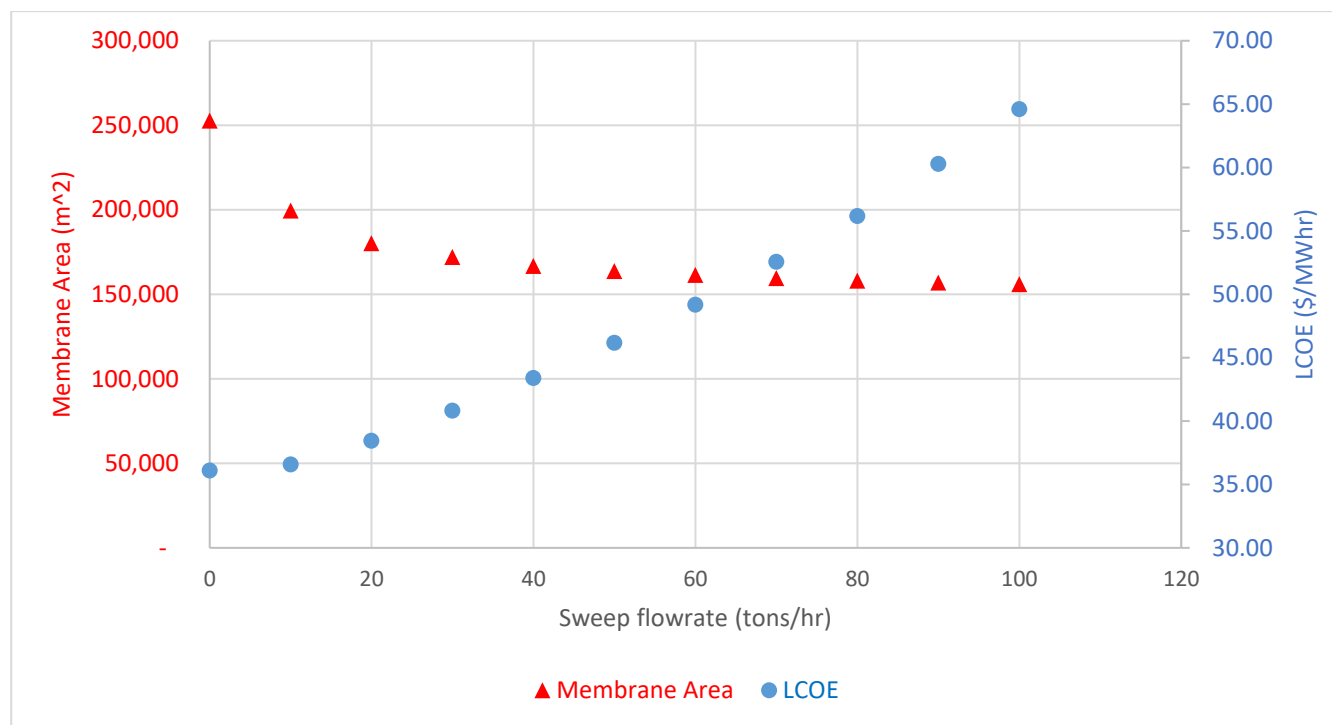
Appendix 7: Detailed compressor and drive cost information for case A optimal case

Compressor	Size (kW)	Compressor Base Equipment Cost ($)	Bare Moule Cost ($)	Drive Base Equipment Cost ($)	Drive Bare Module Cost ($)	Bare Module Cost ($)	Additional Module Cost ($)	GrassRoots Cost ($)	Total Module Costs ($)
1	1,970	688,277	3,957,594	232,083	348,124	4,305,719	775,029.34	460,180.08	**5,540,928**
2	1,970	688,277	3,957,594	232,083	348,124	4,305,719	775,029.34	460,180.08	**5,540,928**
3	1,890	668,991	3,846,698	229,808	344,711	4,191,409	754,453.63	449,399.26	**5,395,262**
4	1,890	668,991	3,846,698	229,808	344,711	4,191,409	754,453.63	449,399.26	**5,395,262**
5	1,730	629,305	3,618,503	224,825	337,238	3,955,741	712,033.44	427,065.15	**5,094,840**
6	1,730	629,305	3,618,503	224,825	337,238	3,955,741	712,033.44	427,065.15	**5,094,840**
7	1,630	603,688	3,471,209	221,380	332,070	3,803,279	684,590.28	412,534.41	**4,900,404**
8	1,500	569,363	3,273,838	216,459	324,688	3,598,527	647,734.80	392,911.03	**4,639,172**
9	1,470	561,267	3,227,283	215,244	322,866	3,550,150	639,026.95	388,255.43	**4,577,432**
10	1,470	561,267	3,227,283	215,244	322,866	3,550,150	639,026.95	388,255.43	**4,577,432**
11	1,410	544,865	3,132,974	212,717	319,076	3,452,050	621,368.92	378,791.10	**4,452,210**
12	1,410	544,865	3,132,974	212,717	319,076	3,452,050	621,368.92	378,791.10	**4,452,210**
13	1,250	499,669	2,873,099	205,266	307,899	3,180,998	572,579.57	352,467.60	**4,106,045**
14	1,090	452,101	2,599,582	196,567	294,851	2,894,433	520,998.00	324,334.28	**3,739,766**

Appendix 8: Detailed cost information of heat exchangers for configuration A optimal case

	Area (m^2)	Duty (kW)	Base Equipment Cost ($)	Bare Module Cost ($)	Total Module Cost ($)
1	980	7,056	115,318	692,194	874,448
2	980	7,056	115,318	692,194	874,448
3	980	7,056	115,318	692,194	874,448
4	940	6,768	112,135	673,091	850,315
5	850	6,120	104,913	629,740	795,550
6	850	6,120	104,913	629,740	795,550
7	810	5,832	101,672	610,289	770,977
8	810	5,832	101,672	610,289	770,977
9	700	5,040	92,644	556,095	702,514
10	700	5,040	92,644	556,095	702,514
11	680	4,896	90,981	546,115	689,907
12	680	4,896	90,981	546,115	689,907
13	600	4,320	84,254	505,732	638,891
14	600	4,320	84,254	505,732	638,891
15	570	4,104	81,695	490,373	619,488
16	570	4,104	81,695	490,373	619,488

Appendix 9: Detailed cost information of membranes in configuration A

Membrane	Size	Total Cost ($)
1	113,600	8,520,000
2	106,100	7,957,500

Appendix 10: Detailed compressor and drive cost information for configuration B optimal case

Compressor	Size (kW)	Compressor Base Equipment Cost ($)	Bare Moule Cost ($)	Drive Base Equipment Cost ($)	Drive Bare Module Cost ($)	Bare Module Cost ($)	Additional Module Cost ($)	Grassroots Cost ($)	Total Module Costs ($)
1	1,910	673,846	3,874,614	230,389	345,584	4,220,198	759,635.60	452,117.51	5,431,951
2	1,910	673,846	3,874,614	230,389	345,584	4,220,198	759,635.60	452,117.51	5,431,951
3	1,770	639,372	3,676,387	226,129	339,193	4,015,581	722,804.52	432,750.30	5,171,135
4	1,770	639,372	3,676,387	226,129	339,193	4,015,581	722,804.52	432,750.30	5,171,135
5	1,670	614,014	3,530,580	222,792	334,187	3,864,767	695,658.11	418,402.72	4,978,828
6	1,630	603,688	3,471,209	221,380	332,070	3,803,279	684,590.28	412,534.41	4,900,404
7	1,540	580,054	3,335,310	218,031	327,046	3,662,356	659,224.11	399,042.31	4,720,623
8	1,490	566,672	3,258,364	216,057	324,086	3,582,450	644,840.95	391,364.69	4,618,655
9	1,490	566,672	3,258,364	216,057	324,086	3,582,450	644,840.95	391,364.69	4,618,655
10	1,430	550,364	3,164,591	213,574	320,362	3,484,953	627,291.55	381,969.07	4,494,214
11	1,430	550,364	3,164,591	213,574	320,362	3,484,953	627,291.55	381,969.07	4,494,214
12	1,300	514,032	2,955,684	207,715	311,572	3,267,256	588,106.02	360,873.34	4,216,235
13	1,170	476,204	2,738,174	201,092	301,638	3,039,812	547,166.17	338,648.04	3,925,626

Appendix 11: Detailed cost information on configuration A optimal case

	Area (m^2)	Duty (kW)	Base Equipment Cost ($)	Bare Module Cost ($)	Total Module Cost ($)
1	990	7,128	116,111	696,956	880,464
2	990	7,128	116,111	696,956	880,464
3	990	7,128	116,111	696,956	880,464
4	880	6,336	107,330	644,251	813,882
5	850	6,120	104,913	629,740	795,550
6	830	5,976	103,295	620,030	783,283
7	690	4,968	91,814	551,111	696,217
8	690	4,968	91,814	551,111	696,217
9	690	4,968	91,814	551,111	696,217
10	690	4,968	91,814	551,111	696,217
11	600	4,320	84,254	505,732	638,891
12	600	4,320	84,254	505,732	638,891
13	580	4,176	82,550	495,507	625,974
14	580	4,176	82,550	495,507	625,974
15	220	1,584	49,322	296,054	374,005

Appendix 12: Detailed cost information on configuration B optimal case

Membrane	Size	Total Cost ($)
1	130,200	9,756,000
2	113,700	8,527,000

Appendix 13: Configuration A with mapping of key variables and assumptions.
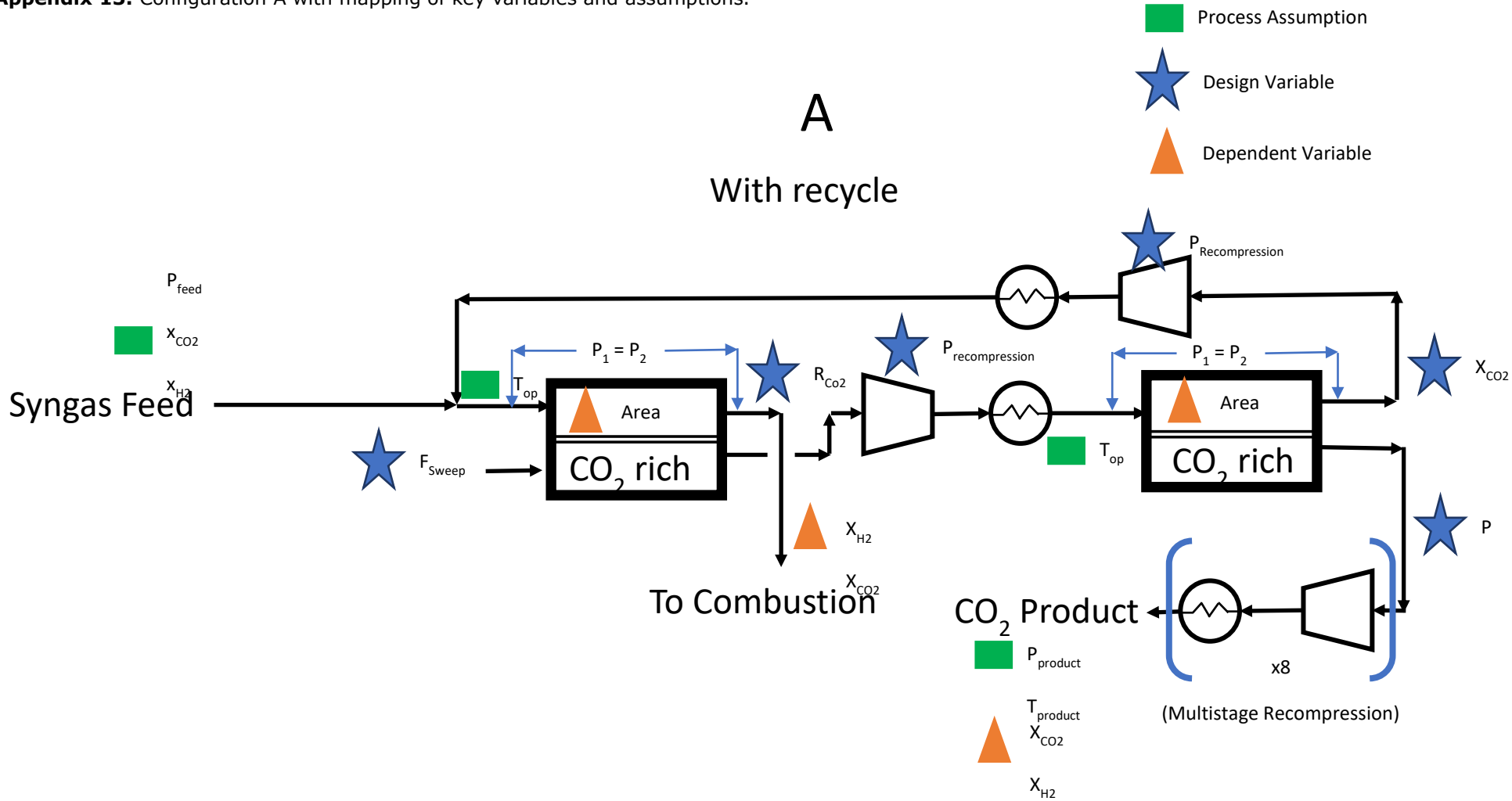
Appendix 14: Configuration B with mapping of key variables and assumptions.
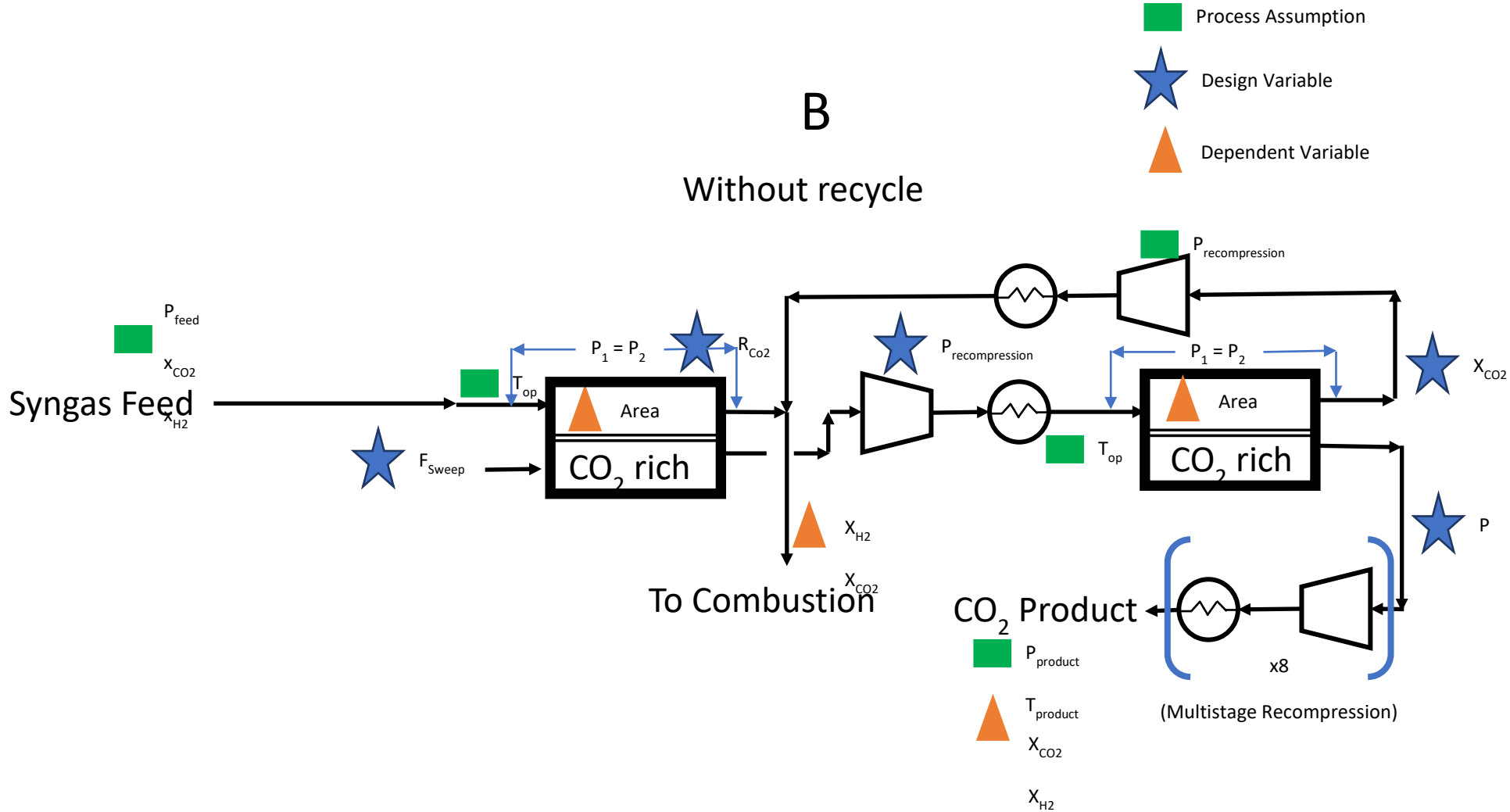
Appendix 15: Discounted Cash Flow For Configuration A Minimum Cost Scenario

Investment ($)	2.25E+08										
Cost of Land ($)	300,000										
Tax Rate	0.25										
	Input Criteria					CO2 Metrics			LCOE Calculation		
	Discount Factor	0.12							Namplate Capacity		634
	Net Present Value (millions)		(0.00)			Carbon Captured (tons)	3,012,058		CO2 Power Usage (MW)		111
	Cost of Capital	0.06				Price Per ton CO2 ($)	0.00		Hours Per Year		7008
						Annual CO2 Revenue ($)	0.00		Annual Capacity (MWhr)		3,665,394
									Price ($/MWhr)		$ 38.66
									Annual Revenue		141,685,843
						Net Capacity (MW)	523		Cumulative NPV		(0.00)

Year	Investment	Depreciat	FCl-Sdk	Revenue	Operating Costs	Membrane	Formula (see Ca	Cash Flow (Non-Discount)	Cash Flow (Disco	Cumulative Cash	Cumulative Cash Flow (discount)
0			225.5								
0	0.3		225.5					(0)	(0)	(0)	(0)
1	79.7		225.5					(80)	(71)	(80)	(71)
2	84.5		225.5					(84)	(67)	(147)	(139)
3	89.5		225.5					(90)	(64)	(211)	(202)
4		22.5	202.9	142	98		39	39	25	(186)	(178)
5		22.5	180.4	142	98		39	39	22	(164)	(156)
6		22.5	157.8	142	98		39	39	20	(145)	(136)
7		22.5	135.3	142	98		39	39	18	(127)	(119)
8		22.5	112.7	142	98		39	39	16	(112)	(103)
9		22.5	90.2	142	98	33	14	14	5	(107)	(98)
10		22.5	67.6	142	98		39	39	12	(94)	(86)
11		22.5	45.1	142	98		39	39	11	(83)	(75)
12		22.5	22.5	142	98		39	39	10	(73)	(65)
13		22.5	-	142	98		39	39	9	(64)	(56)
14				142	98	33	14	14	3	(61)	(53)
15				142	98		39	39	7	(54)	(46)
16				142	98		39	39	6	(48)	(40)
17				142	98		39	39	6	(42)	(34)
18				142	98		39	39	5	(37)	(29)
19				142	98	33	14	14	2	(36)	(27)
20				142	98		39	39	4	(32)	(23)
21				142	98		39	39	4	(28)	(20)
22				142	98		39	39	3	(25)	(16)
23				142	98		39	39	3	(22)	(14)
24				142	98	33	14	14	1	(21)	(13)
25				142	98		39	39	2	(19)	(10)
26				142	98		39	39	2	(17)	(8)
27				142	98		39	39	2	(15)	(7)
28				142	98		39	39	2	(13)	(5)
29				142	98	33	14	14	1	(13)	(4)
30				142	98		39	39	1	(12)	(3)
31				142	98		39	39	1	(10)	(2)
32				142	98		39	39	1	(9)	(1)
33				142	98		39	39	1	(9)	(0)

Appendix 16: Performance parameters for membrane system

Parameter	Target	Selexol Baseline
H_2 recovery	>=95%	99.8%
CO_2 recovery	>=90%*	90.0%*
H_2 purity	>=85%	91.2%
CO_2 purity	>=95%	99.0%
$X_{H2O, CO2\ product}$	<500 ppm	500 ppm

Appendix 17: Program used to calculate costs more quickly

```
Public i As Integer

Public MaxIt As Integer

Public j As Integer

Public memcost As Integer

Public disc As Double


 'identifies how many rows need to be calculated

Sub Numberofrows()

    Sheets("Data Sheet").Select

    MaxIt = Range("AY1").Value

    MsgBox ("There will be " & MaxIt & " rows of cost calculated") 'prompt for costing iterations to indicate how
many operations are run

End Sub
```

```vba
'overall costing calculation
Sub RapidCost()
i = 0
Call Numberofrows
Do
If i < MaxIt Then
    Sheets("Data Sheet").Select
    Range(Cells((i + 1), 1), Cells((i + 1), 1)).Select
    Call CopyValues ' takes from data sheet to the respective costing sheets
    Call RunningSolver 'calculates LCOE
    Call PasteValues ' Takes capital cost, operating costs, and LCOE and puts back on data sheet
    i = i + 1
End If
Loop While i < MaxIt 'loops until the total number of rows are calculated
End Sub



' Copies values to the input sheet
Sub CopyValues()
'selecting the cells of interest for compressors
    Sheets("Data Sheet").Select
   ' Range("T2:AE2").Select
   Range(Cells((i + 2), 20), Cells((i + 2), 31)).Select 'index of row with compressor power values
```

```vba
Selection.Copy

Sheets("Input").Select

Application.Run "getUnits"

Range("A2").Select 'pasting into compressor input

ActiveSheet.Paste

  'getting heatex values

Sheets("Data Sheet").Select

Application.Run "getUnits"

Range(Cells(i + 2, 32), Cells(i + 2, 41)).Select 'index of row with heatex values

Application.CutCopyMode = False

Selection.Copy

Sheets("Input").Select

Application.Run "getUnits"

Range("A6").Select 'selecting paste destination for heatex data

ActiveSheet.Paste

'getting membrane values

Sheets("Data Sheet").Select

Application.Run "getUnits"

Range(Cells(i + 2, 18), Cells(i + 2, 19)).Select ' index of row for membrane values

Application.CutCopyMode = False

Selection.Copy

Sheets("Input").Select

Application.Run "getUnits"
```

```vba
    Range("A9").Select ' pasting membrane values

    ActiveSheet.Paste

    Sheets("Data Sheet").Select

    Application.Run "getUnits"

        'getting CO2 metrics values

    Sheets("Data Sheet").Select

    Application.Run "getUnits"

    Range(Cells(i + 2, 13), Cells(i + 2, 13)).Select ' index of row for CO2 capture values

    Application.CutCopyMode = False

    Selection.Copy

    Sheets("Input").Select

    Application.Run "getUnits"

    Range("A12").Select ' pasting Co2 capture value

    ActiveSheet.Paste

    Sheets("Data Sheet").Select

    Application.Run "getUnits"
End Sub



Sub RunningSolver()
'
' RunningSolver Macro
' Short macro to run the solver
```

```
'
 Sheets("Cashflow").Select
'Selects the flowsheet
    SolverOk SetCell:="$E$7", MaxMinVal:=3, ValueOf:=0, ByChange:="$M$10", Engine:= _
        1, EngineDesc:="GRG Nonlinear"
    SolverOk SetCell:="$E$7", MaxMinVal:=3, ValueOf:=0, ByChange:="$M$10", Engine:= _
        1, EngineDesc:="GRG Nonlinear"
  SolverSolve (True) 'closes dialog box
End Sub


Sub PasteValues()
' Pasting values from output sheet to data sheet

'Pasting the Capital Costs
    Sheets("Output").Select
    Application.Run "getUnits"
    Range("B6").Select
    Selection.Copy
    Sheets("Data Sheet").Select
    Application.Run "getUnits"
    'Range("AT2").Select
    Cells(i + 2, 46).Select ' Pasting into indexed location
    Selection.PasteSpecial Paste:=xlPasteValues, Operation:=xlNone, SkipBlanks _
```

```
        :=False, Transpose:=False
'Pasting the Operating Costs
    Sheets("Output").Select

    Application.Run "getUnits"

    Range("B9").Select

    Application.CutCopyMode = False

    Selection.Copy

    Sheets("Data Sheet").Select

    Application.Run "getUnits"

    ' Range("AU2").Select

   Cells(i + 2, 47).Select ' Pasting into indexed location

    Selection.PasteSpecial Paste:=xlPasteValues, Operation:=xlNone, SkipBlanks _

        :=False, Transpose:=False

    Sheets("Output").Select
'Pasting the LCOE
    Application.Run "getUnits"

    Range("B11").Select

    Application.CutCopyMode = False

    Selection.Copy

    Sheets("Data Sheet").Select

    Application.Run "getUnits"

    '  Range("AV2").Select

   Cells(i + 2, 48).Select ' Pasting into indexed location
```

```vba
    Selection.PasteSpecial Paste:=xlPasteValues, Operation:=xlNone, SkipBlanks _
        :=False, Transpose:=False
    Range("AU5").Select
    'Pasting the CO2 capture metric
    Sheets("Output").Select
    Application.Run "getUnits"
    Range("B17").Select
    Selection.Copy
    Sheets("Data Sheet").Select
    Application.Run "getUnits"
    'Range("AT2").Select
    Cells(i + 2, 49).Select ' Pasting into indexed location
    Selection.PasteSpecial Paste:=xlPasteValues, Operation:=xlNone, SkipBlanks _
        :=False, Transpose:=False
End Sub

Sub pastesensitivity()
    ' Copying the LCOE
    Sheets("Output").Select
    Application.Run "getUnits"
    Range("B11").Select
    Selection.Copy
    Sheets("Sens").Select
```

```vba
 Application.Run "getUnits"
 'Range("AT2").Select
 Cells(j + 2, 3).Select ' Pasting into indexed location
 Selection.PasteSpecial Paste:=xlPasteValues, Operation:=xlNone, SkipBlanks _
     :=False, Transpose:=False
' Copying the CO2 sales price
 Sheets("Output").Select
 Application.Run "getUnits"
 Range("B17").Select
 Selection.Copy
 Sheets("Sens").Select
 Application.Run "getUnits"
 'Range("AT2").Select
 Cells(j + 2, 4).Select ' Pasting into indexed location
 Selection.PasteSpecial Paste:=xlPasteValues, Operation:=xlNone, SkipBlanks _
     :=False, Transpose:=False
' Copying the CO2 penalty price
 Sheets("Output").Select
 Application.Run "getUnits"
 Range("B18").Select
 Selection.Copy
 Sheets("Sens").Select
 Application.Run "getUnits"
```

```vba
    'Range("AT2").Select

    Cells(j + 2, 5).Select ' Pasting into indexed location

    Selection.PasteSpecial Paste:=xlPasteValues, Operation:=xlNone, SkipBlanks _
        :=False, Transpose:=False
End Sub


Sub memcostmodify()
'modifies membrane cost for sensitivity analysis



'Selecting index
    Sheets("Sens").Select
   ' Range("T2:AE2").Select
  Range(Cells((j + 2), 2), Cells((j + 2), 2)).Select 'index of row with compressor power values
    Selection.Copy
    Sheets("Membrane").Select
    Application.Run "getUnits"
    Range("A4").Select 'pasting into compressor input
    ActiveSheet.Paste
End Sub


Sub discountmodify()
'modify discount rate for sensitivity analysis
```

```vba
    Sheets("Sens").Select
    ' Range("T2:AE2").Select
   Range(Cells((j + 2), 2), Cells((j + 2), 2)).Select 'index of row with compressor power values
    Selection.Copy
    Sheets("CashFlow").Select
    Application.Run "getUnits"
    Range("C6").Select 'pasting into discount rate input
    ActiveSheet.Paste




End Sub



Sub Sensmem()
j = 0
 Sheets("Sens").Select
     MaxJ = Range("J1").Value
      Sheets("Membrane").Select
  memcost = Range("A4").Value
    MsgBox ("There will be " & memcost & " iterations")
```

```
Do

If j < MaxJ Then

i = 0

Call CopyValues

Call memcostmodify

Call RunningSolver

Call PasteValues

Call pastesensitivity

j = j + 1

End If


Loop While j < MaxJ

    MsgBox ("This sub is complete after " & MaxJ & " iterations")

 Sheets("Membrane").Select

   Range("A4").Value = memcost

End Sub


Sub Sensdisc()
'sensitivity analysis for discount rate


j = 0

 Sheets("Sens").Select

    MaxJ = Range("J1").Value
```

```vba
    Sheets("Cashflow").Select
  disc = Range("C6").Value
    MsgBox ("There will be " & MaxJ & " iterations")
Do
If j < MaxJ Then
i = 0
Call CopyValues
Call discountmodify
Call RunningSolver
Call PasteValues
Call pastesensitivity
j = j + 1
End If
Loop While j < MaxJ
    MsgBox ("This sub is complete after " & disc & " iterations")
 Sheets("Cashflow").Select
    Range("C6").Value = disc
End Sub
```